



UPPSALA  
UNIVERSITET

UPTEC W 18 006

Examensarbete 30 hp  
Juni 2018

# Point source carbon capture by porous inorganic carbonates

Kolavskiljning från punktkälla med porösa  
oorganiska karbonater

---

Jonas Hultberg



## Abstract

### Point source carbon capture by porous inorganic carbonates

Jonas Hultberg

Mesoporous inorganic carbonates (MIC) was synthesized and tested as adsorbents for CO<sub>2</sub>, using vacuum and temperature swing adsorption. Mesoporous magnesium carbonate (MMC), mesoporous calcium carbonate (MCC) and mesoporous calcium magnesium carbonate (MCMC), all included in MIC, are exceedingly porous with an amorphous structure. MMC was first reported in 2013, where it was synthesized in a methanol and MgO mixture under CO<sub>2</sub> pressure. In this work, the synthesis of MCC and MCMC was developed from the synthesis of MMC. Further effects on the CO<sub>2</sub> adsorption characteristics of the MIC materials with several additives (Al(NO<sub>3</sub>)<sub>3</sub>, Al<sub>2</sub>O<sub>3</sub>, K<sub>2</sub>CO<sub>3</sub> and KNO<sub>3</sub>) introduced into the porous structures were also investigated.

The MCC materials CO<sub>2</sub> adsorption capacity (14.96 mmol g<sup>-1</sup>) was drastically lowered (7.29 mmol g<sup>-1</sup>) by severe sintering after continuous cycles when heat was used for sorbent regeneration. The combined structure of MCMC improved the stability, mitigating the sintering for high temperature adsorption/desorption (650 °C, 850 °C). The addition of Al(NO<sub>3</sub>)<sub>3</sub> improved the stability further, with an optimum additive amount of 35 wt.%, giving a high initial CO<sub>2</sub> uptake (12.23 mmol g<sup>-1</sup>) and maintaining a high CO<sub>2</sub> uptake after 23 cycles (10.96 mmol g<sup>-1</sup>).

The pure gas CO<sub>2</sub> uptake of MMC was around 1.52 mmol g<sup>-1</sup> at 101 kPa (0 °C) using vacuum swing adsorption. The N<sub>2</sub> uptake under the same conditions was less than 0.10 mmol g<sup>-1</sup>. All of the additives tested increased the CO<sub>2</sub> uptake of MIC under these conditions, with the most promising additives being low weight percentages of potassium carbonate (5-10 wt.%) added to MMC for low temperature adsorption (0 °C). The incorporation of 5 wt.% K<sub>2</sub>CO<sub>3</sub> increased the CO<sub>2</sub> uptake of MMC up to 3.24 mmol g<sup>-1</sup>, suggesting that the required energy for adsorption on this sample, due to the sorbent surpassing 3 mmol g<sup>-1</sup> CO<sub>2</sub> capacity, could be less than for conventional chemical adsorbents.

Vacuum swing cyclic CO<sub>2</sub> adsorption/desorption showed a decrease in CO<sub>2</sub> uptake on MMC with 5 wt.% K<sub>2</sub>CO<sub>3</sub> after each cycle. Heat regeneration (150 °C, for 30 minutes) could recover most of the lost CO<sub>2</sub> capacity each cycle. Heat indicatively improved the cyclic performance of this adsorbent without damaging the nanoporous structure. MMC with 5 wt.% K<sub>2</sub>CO<sub>3</sub> was the best performing adsorbent when vacuum was used for sorbent regeneration and can potentially be further developed into a good CO<sub>2</sub> adsorbent for temperature swing adsorption (TSA) processes.

**Keywords:** Carbon capture, Gas separation, Adsorbent, Inorganic carbonates, Point source, Carbon dioxide

---

Department of Engineering Sciences, Nanotechnology and Functional Materials, Uppsala University (UU), Ångström laboratory, Lägerhyddsvägen 1, Box 534, SE-751 21 Uppsala, Sweden

## Referat

### Kolavskiljning från punktkälla med porösa oorganiska karbonater

Jonas Hultberg

Porösa oorganiska karbonater (MIC) syntetiserades och testades som adsorbenter för CO<sub>2</sub>, med vakuum- och temperaturskiftesadsorption. Mesoporöst magnesiumkarbonat (MMC), mesoporöst kalciumkarbonat (MCC) och mesoporöst kalciummagnesiumkarbonat (MCMC), som alla ingår i MIC, är mycket porösa med en amorf struktur. MMC rapporterades som tidigast 2013, där det syntetiserades i en metanol- och MgO-blandning under koldioxidtryck. Syntesen av MCC och MCMC utvecklades från syntesen av MMC. Effekterna på adsorptionsegenskaperna för CO<sub>2</sub> på MIC-materialen undersöktes ytterligare med flera tillsatser (Al(NO<sub>3</sub>)<sub>3</sub>, Al<sub>2</sub>O<sub>3</sub>, K<sub>2</sub>CO<sub>3</sub> och KNO<sub>3</sub>) som tillfördes de porösa strukturerna.

MCC-materialets adsorptionskapacitet för CO<sub>2</sub> (14,96 mmol g<sup>-1</sup>) sänktes drastiskt till 7,29 mmol g<sup>-1</sup> på grund av intensiv vittring under kontinuerliga cykler när värme användes för återvinning av sorbenten. Den kombinerade strukturen hos MCMC förbättrade stabiliteten och lindrade vittringen för adsorption/desorption vid hög temperatur (650 ° C, 850 ° C). Tillsatsen av Al(NO<sub>3</sub>)<sub>3</sub> förbättrade stabiliteten ytterligare, med en optimal tillsats av 35 vikt%. Då gavs ett högt initialupptag av CO<sub>2</sub> (12,23 mmol g<sup>-1</sup>) och det upprätthölls ett högt upptag efter 23 cykler (10,96 mmol g<sup>-1</sup>).

Det rena gasupptaget av CO<sub>2</sub> på MMC var omkring 1,52 mmol g<sup>-1</sup> vid 101 kPa (0 ° C) med vakuumskiftesadsorption. Kväveupptaget under samma förhållanden var mindre än 0,10 mmol g<sup>-1</sup>. Alla tillsatser hade en ökande effekt på upptaget av CO<sub>2</sub> på MIC under dessa förhållanden, varvid de mest lovande tillsatserna var låga viktprocenter av K<sub>2</sub>CO<sub>3</sub> (5–10 vikt%) tillförda MMC för adsorption vid låg temperatur (0 ° C). Tillförandet av 5 vikt% K<sub>2</sub>CO<sub>3</sub> ökade upptaget på MMC till 3,24 mmol g<sup>-1</sup> CO<sub>2</sub>, vilket kan antyda att energin som krävs för adsorption på detta prov är mindre än för konventionella kemiska adsorbenter.

Vakuumsiftning för cyklisk adsorption/desorption av CO<sub>2</sub> visade en minskning i upptag på MMC tillfört 5 vikt% K<sub>2</sub>CO<sub>3</sub> efter varje cykel. En applicering av värme för sorbentåtervinning (150 ° C, i 30 minuter) kunde återfå majoriteten av den förlorade kapaciteten efter varje cykel. Värme förbättrade signifikant den cykliska prestandan hos denna adsorbent, utan att skada dess nanoporösa struktur. MMC tillfört 5 vikt% K<sub>2</sub>CO<sub>3</sub> var den bästa adsorbenten när vakuum användes för sorbentåtervinning och kan potentiellt vidareutvecklas till en effektiv adsorbent för processer med temperaturskifte (TSA).

**Nyckelord:** Kolavskiljning, Adsorbenter, Oorganiska karbonater, Punktkälla, Koldioxid

## **Preface**

This work concludes the master program in Environmental and Water Engineering at Uppsala University. The work has been done at the division for Nanotechnology and Functional materials with Ocean Cheung as supervisor and it comprises 30 credits. Maria Strømme, professor at the division of Nano Technology and Functional materials, Department of Engineering Sciences, has been the subject reader.

I would like to thank my supervisor Ocean Cheung for all the guidance and expert advice in this work, it has been very rewarding working with you. I would also like to thank Maria Wall for all the help in the laboratory, with XRD and SEM analysis and for enduring working together using the oven in the cellar, you have been a great support both as a friend and colleague. I have also received help and support from Rui Sun regarding samples and experiments, thank you. Finally, I would like to thank my subject reader Maria Strømme for the work opportunities she has given me at NFM and for the help with the report.

Jonas Hultberg

Uppsala, juni 2018

---

Copyright© Jonas Hultberg and the Department of Engineering Sciences,  
Nanotechnology and Functional Materials.

UPTEC W 18 006, ISSN 1401-5765

Published digitally at the Department of Earth Sciences, Uppsala University 2018.

## Populärvetenskaplig sammanfattning

### Kolavskiljning från punktkälla med porösa oorganiska karbonater

Jonas Hultberg

Koldioxidutsläpp från antropogena källor som ackumuleras i atmosfären skapar större miljöproblem än någonsin genom klimatförändringar. Det är troligt att fossila bränslen kommer att fortsätta att vara den främsta energikällan inom den närmsta framtiden. Koldioxid är den näst viktigaste växthusgasen efter vattenånga och står för 77% av det antropogena bidraget till växthuseffekten och därför är en minskning av koldioxidutsläpp av stor betydelse och brådskande behov.

Fortlöpande arbete pågår inom akademien för att hitta metoder som minskar koldioxidutsläppen. En av dessa metoder är kolavskiljning från stora punktkällor, till exempel industrier eller kolkraftverk. Med en separering av koldioxid från emissioner redan vid produktions- eller förbränningssteget har kolavskiljning potential att vara ett effektivt sätt att sänka de globala koldioxidutsläppen. Avskiljningsdelen är den första processen i geologisk lagring av koldioxid eller carbon capture and storage (CCS), som består av tre steg: Avskiljning, transport och lagring. Avskiljningsprocessen är idag dyrast (upp till 50 € / ton CO<sub>2</sub>) medan lagringen till och med kan vara lönsam. Därför är avskiljningen en stor del av CCS.

Kolavskiljning kan ske genom adsorptionsprocesser och för att det ska fungera behövs ett lämpligt adsorptionsmaterial. Material som är lämpliga för en effektiv kolavskiljning behöver flera egenskaper såsom en hög adsorptionskapacitet, ett snabbt upptag, rimliga adsorptionstemperaturer och cyklisk stabilitet. Den separerade koldioxiden kan i sin tur injiceras i gamla oljereservoarer för förvaring och för att få en ökad oljeutvinning. Koldioxiden kan också användas i livsmedel och kemiska industrier runt om i världen, såsom kolsyrade drycker och gödselproduktion.

Idag finns det flera tekniker som undersöks för koldioxidavskiljning från emissioner, däribland absorption och adsorption, där absorption till störst utsträckning är implementerad idag. I absorptionsprocessen kyls gaserna innehållande koldioxid och blandas i ett lösningsmedel. Lösningensmedlet reagerar med koldioxiden som bildar en svagt bunden förening. För avskiljning hettas lösningen upp, som då avlägsnar koldioxiden. Detta återvinner lösningensmedlet, som vidare kyls för fortsatt absorption.

I detta arbete undersöker vi adsorptionsprocesser som använder tryck/vakuum eller temperatur för adsorption-/desorptionscykler av koldioxid på en materialyta. Dessa adsorptionsbaserade teknologier är tryck-/vakuumsiftesadsorption (PSA/VSA) och temperatursiftesadsorption (TSA). Där skillnaden är strategin för återvinningen av adsorptionsmaterialet. Adsorptionsprocesser skulle kunna minska den energi och kostnad som krävs för separationen av koldioxid från förbränningsgaser.

Material som aktivt kol, zeoliter, aluminiumoxid, alkalimetallkarbonater och hydrotalcitföreningar (HTlcs) har redan utvecklats som konventionella adsorbenter för att selektivt och reversibelt fungera som kolavskiljare från emissioner.

I detta arbete undersöks möjligheten för mesoporösa oorganiska karbonater (MIC) att avskilja koldioxid vid temperaturer som är relevanta för industrier eller kolkraftverk. Syftet är att optimera MIC, som inkluderar mesoporöst magnesiumkarbonat (MMC), mesoporöst kalciumkarbonat (MCC) och mesoporöst kalcium-magnesiumkarbonat (MCMC), som kandidater till kolavskiljning från punktkällor. Denna optimering utförs av tillsatsmaterial (Al(NO<sub>3</sub>)<sub>3</sub>, Al<sub>2</sub>O<sub>3</sub>, K<sub>2</sub>CO<sub>3</sub> och KNO<sub>3</sub>) som tillförs till syntesprocessen av MIC-materialen. I arbetet övervägs också effekterna som tillsatserna har på MIC gällande stabilitet, för att förhindra vittring över kontinuerliga cykler av

koldioxidadsorption och desorption. Konventionella material, MMC, MCC och MCMC används sedan som referenser för att förbättra egenskaperna hos MIC med avseende på koldioxidavskiljning.

Adsorptionsmaterialens prestanda testas experimentellt av VSA och TSA samt undersöks analytiskt genom röntgendiffraktion (XRD) för morfologi, kväve adsorption med Brunauer-Emmett-Teller (BET) för ytaarea/porositet och svepelektronmikroskop (SEM) för detaljerade strukturbilder av nanopartikelytor.

MIC med hög porositet och ytaarea kunde framställas framgångsrikt tillsammans med tillsatsmaterial. Analyser visade att MIC förblev röntgenamorfa efter tillförandet av tillsatsmaterialen och att de fortfarande hade en nanoporös struktur, dock med en minskning i ytaarea.

Cykliska tester med temperaturskifte visade att MCC-materialets adsorptionskapacitet av koldioxid sänktes drastiskt på grund av intensiv vittring när värme användes för materialåtervinning. Den kombinerade strukturen hos MCMC kunde förbättra stabiliteten och lindra denna vittring. Tillsatsen av  $\text{Al}(\text{NO}_3)_3$  förbättrade stabiliteten ytterligare, där den optimala tillsatsen visade sig vara 35 vikt%. Tillsatsen gav en hög adsorptionskapacitet som kunde upprätthållas relativt bra efter 23 cykler.

Alla tillsatser visades ge en ökande effekt på upptaget av koldioxid på MIC med vakuumsiftesadsorption. Den mest lovande tillsatsen var 5 vikt%  $\text{K}_2\text{CO}_3$  tillfört MMC för adsorption vid låg temperatur. Tillsatsmaterialet visades öka upptaget på MMC till över det dubbla jämfört med innan. Cykliska tester med vakuumskifte visade en minskning i upptag på MMC med  $\text{K}_2\text{CO}_3$ -tillsatsen efter varje cykel. Värme kunde dock återfå majoriteten av den förlorade kapaciteten. Materialet visade en förbättring i cyklisk prestanda utan att dess nanoporösa struktur skadades.

MMC tillsatt  $\text{K}_2\text{CO}_3$  kan vidareutvecklas som en adsorbent för användning i temperaturskiftesprocesser. MCMC kan ytterligare optimeras med lägre kalciumhalter och tillsatser av kalium eller aluminium för kolavskiljning vid lägre temperaturer.

Resultaten i detta arbete kan användas för att ytterligare optimera adsorptionstekniker för koldioxidavskiljning från emissioner i industrier och kraftverk. Effektiva adsorbenter kan utnyttjas för att minska den energi som krävs i kolavskiljningsprocesser. Detta för att minska koldioxiden i atmosfären och därmed minska effekterna av klimatförändringarna.

## **Abbreviations**

**ASAP** – Accelerated Surface Area and Porosimetry analysis

**BET** – Brunauer-Emmet-Teller

**CCS** – Carbon Capture and Storage

**MCC** – Mesoporous Calcium Carbonate

**MCMC** – Mesoporous Calcium-Magnesium Carbonate

**MIC** – Mesoporous Inorganic Carbonates

**MMC** – Mesoporous Magnesium Carbonate

**SEM** – Scanning Electron Microscope

**TGA** – Thermogravimetric analysis

**TSA** – Temperature Swing Adsorption

**VSA** – Vacuum Swing Adsorption

**XRD** – X-ray Diffraction

## **Glossary**

**Calcination/calciner** – Thermal decomposition of carbonates to give carbon dioxide

**Carbonation/carbonator** – Reactions of carbon dioxide to give carbonates

**Kinetics** – Chemical reaction rates

**Sintering** – Compacting and forming a solid mass of material by heat or pressure

**Synthesis** – The production of chemical compounds by reaction from simpler materials

## Contents

1.	INTRODUCTION .....	1
1.1.	BACKGROUND.....	1
1.2.	AIM .....	1
1.3.	CARBON CAPTURE TECHNIQUES .....	2
1.4.	MECHANISMS OF ADSORPTION.....	3
1.4.1.	Chemisorption .....	3
1.4.2.	Physisorption.....	3
1.5.	SWING ADSORPTION.....	3
1.5.1.	Temperature swing adsorption (TSA).....	3
1.5.2.	Pressure/Vacuum swing adsorption (PSA/VSA).....	4
1.6.	ADSORBENT MATERIALS.....	4
1.6.1.	Low temperature sorbents.....	5
1.6.2.	Intermediate temperature sorbents .....	5
1.6.3.	High temperature sorbents .....	5
1.7.	MESOPOROUS INORGANIC CARBONATES (MIC).....	5
2.	MATERIALS AND METHODS.....	7
2.1.	MATERIALS.....	7
2.1.1.	Base materials .....	7
2.1.2.	Reference materials .....	7
2.1.3.	Additives – Thermal stability and sintering.....	7
2.2.	SYNTHESIS .....	8
2.2.1.	Mesoporous magnesium carbonate (MMC) .....	8
2.2.2.	Mesoporous calcium carbonate (MCC).....	8
2.2.3.	Mesoporous calcium magnesium carbonate (MCMC).....	8
2.2.4.	Mesoporous magnesium carbonate (MMC) with additives.....	9
2.2.5.	Mesoporous calcium magnesium carbonate (MCMC) with additives.....	9
2.3.	ANALYTICAL TECHNIQUES FOR CHARACTERIZATION .....	9
2.3.1.	Powder X-ray diffraction (XRD) .....	9
2.3.2.	Volumetric gas adsorption (BET) .....	9
2.3.3.	Scanning electron microscope (SEM).....	9
2.4.	CARBON CAPTURE TECHNIQUES .....	10
2.4.1.	Temperature swing adsorption (TSA).....	10
2.4.2.	Vacuum swing adsorption (VSA) .....	10
3.	RESULTS AND DISCUSSION.....	12
3.1.	CHARACTERIZATION.....	12
3.1.1.	Morphology and structure.....	12

3.1.2.	Additive characterization.....	14
3.2.	CO <sub>2</sub> TEMPERATURE SWING ADSORPTION .....	15
3.2.1.	CO <sub>2</sub> adsorption capacity - References .....	16
3.2.2.	CO <sub>2</sub> adsorption capacity - Additives .....	16
3.2.3.	CO <sub>2</sub> temperature swing cycling.....	18
3.2.4.	Adsorption kinetics.....	19
3.3.	CO <sub>2</sub> VACUUM SWING ADSORPTION .....	20
3.3.1.	CO <sub>2</sub> adsorption isotherms - References.....	20
3.3.2.	CO <sub>2</sub> adsorption isotherms - Additives.....	22
3.3.3.	CO <sub>2</sub> vacuum swing cycling.....	27
3.4.	CO <sub>2</sub> CYCLING AT ROOM TEMPERATURE .....	27
3.5.	THERMAL STABILITY AND SINTERING.....	28
4.	CONCLUSIONS .....	32
4.1.	Characterization .....	32
4.2.	Temperature swing adsorption.....	32
4.3.	Vacuum swing adsorption .....	32
5.	FUTURE OUTLOOK.....	33
6.	REFERENCES .....	34

# 1. INTRODUCTION

## 1.1. BACKGROUND

As a greenhouse gas, the continued emission of carbon dioxide from anthropogenic sources cause ever increasing environmental problems due to its accumulation in the atmosphere causing climate change. Environmental impacts from climate change include changing precipitation and the melting of snow/ice which alters hydrological systems and affects water resources (Field et al., 2014). Continued emissions of greenhouse gases can worsen climate change with more climate-related extremes such as heat waves, droughts, cyclones, floods and wildfires (Field et al., 2014). It's likely that in the near future, fossil fuels will continue to be a prominent energy source, with The International Energy Agency (IEA) foreboding fossil fuels to be the dominant energy source until 2030 (Wagner et al., 2016).

CO<sub>2</sub> is the second-most important green-house gas after water vapor, accounting for 77% of the anthropogenic contribution to the green-house effect (30 percent of total CO<sub>2</sub> emissions) (Songolzadeh et al., 2014). Therefore, reducing emissions and thereby atmospheric levels of CO<sub>2</sub> is of great importance and of urgent need.

There is continuous work by the engineering and scientific community for methods on reducing CO<sub>2</sub> emissions. One of these methods is carbon capture from large point sources, such as industries or power plants, averting the emission to the atmosphere. With this approach carbon capture has the potential to be an efficient reducer of global CO<sub>2</sub>-emissions (Haaf et al., 2017).

CO<sub>2</sub> capture can be done by adsorption processes, but a suitable adsorbent is needed for this to work. Materials suitable for an efficient CO<sub>2</sub> capture needs several characteristics such as a high CO<sub>2</sub> adsorption capacity, fast sorption kinetics, industry favorable sorption temperatures and cyclic stability (S. Wang et al., 2011). Carbon capture is the first process in carbon capture and storage (CCS) which consists of three stages: CO<sub>2</sub> separation, transportation and storage. The separation process is today very costly (up to 50 €/ton-CO<sub>2</sub>), while storage can even be profitable with enhanced oil recovery (EOR) (Songolzadeh et al., 2014). This makes the separation of CO<sub>2</sub> a major part of CCS.

Separated CO<sub>2</sub> from carbon capture processes can be injected into oil reservoirs to increase mobility of oil by EOR operations (Songolzadeh et al., 2014). However, the regional potential is not evenly distributed with injection sites located far from CO<sub>2</sub> sources and adding storage-related activities to CO<sub>2</sub>-EOR increases the cost (Juho, 2015; Wagner et al., 2016). CCS has health risks that include asphyxiation and can compromise safe drinking water supplies. Normally CO<sub>2</sub> is a trace gas with a content of around 0.04% in the atmosphere, however, it poses an immediate threat to human life at concentrations of more than 7% (Fogarty and McCally, 2010). Pure CO<sub>2</sub> is used in food/beverages and chemical industries around the world such as fertilizer production, dry ice production and carbonated beverages (Songolzadeh et al., 2014).

## 1.2. AIM

In this work, we will examine the ability for inorganic carbonates to capture CO<sub>2</sub> at different temperatures that are relevant to industries or power plants. The purpose is to optimize MIC, which include MMC, MCC and MCMC, as candidate adsorbents for CO<sub>2</sub> capture from point sources. This optimization will be performed by additive materials

( $\text{Al}(\text{NO}_3)_3$ ,  $\text{Al}_2\text{O}_3$ ,  $\text{K}_2\text{CO}_3$ ,  $\text{KNO}_3$ ) administered to the synthesis of the base materials. The adsorption materials performance will be experimentally tested by vacuum swing adsorption (VSA) and temperature swing adsorption (TSA). Further, the adsorption materials will be characterized analytically by powder X-ray diffraction (XRD) for morphology, BET nitrogen adsorption (BET surface area) (Brunauer et al., 1938) and scanning electron microscope (SEM) for micrographs and morphology of nanoparticle surfaces.

Materials such as activated carbon, zeolite, alumina, MOF, alkali metal carbonates, HTlcs,  $\text{Li}_2\text{ZrO}_3$  and  $\text{Li}_4\text{SiO}_4$  have already been developed as conventional materials to selectively and reversibly act as  $\text{CO}_2$  sorbents from flue gas (Songolzadeh et al., 2014; S. Wang et al., 2011; Xiao et al., 2011). With the goal of optimizing MIC with additives for efficient  $\text{CO}_2$  capture, in this work we consider characteristics of the materials such as high  $\text{CO}_2$  selectivity, high adsorption capacity, favorable operation temperature (0-200 °C, 200-450 °C, 650-850 °C) and fast adsorption kinetics. We also consider the effects of additives on the base materials to prevent sintering for good thermal and mechanical cyclic stability.

Therefore, we will optimize MIC with additives and use the conventional and base materials (MMC, MCC, MCMC) as references to try to improve the material characteristics in regard to  $\text{CO}_2$  adsorption.

### 1.3. CARBON CAPTURE TECHNIQUES

There are three major approaches in carbon capture: post-combustion capture, pre-combustion capture and the oxy-fuel process (Songolzadeh et al., 2014). Post-combustion capture separates  $\text{CO}_2$  from flue gas after combustion with diluted exhaust gas of mostly nitrogen and water in addition to  $\text{CO}_2$  (around 15 %) (Wall, 2007). In pre-combustion capture, gas is synthesized (syngas) which is made up of mostly carbon monoxide and hydrogen. The syngas is reacted with steam to get  $\text{CO}_2$  and more hydrogen. The  $\text{CO}_2$  is then separated often by chemical absorption processes and results in a hydrogen-rich fuel used in furnaces, engines and turbines (Wall, 2007). In the oxy-fuel process, pure oxygen is used for combustion, resulting in a  $\text{CO}_2$ -rich (above 80 vol.%) flue gas which is separated by condensing water (Buhre et al., 2005). The most important technique to prevent  $\text{CO}_2$  emissions is the post-combustion capture. This is because of the flexibility in how to capture the  $\text{CO}_2$  from flue gas, how it can easily be added to fossil fuel power plants and because the main anthropogenic emissions of  $\text{CO}_2$  come from the combustion of fossil fuels (Songolzadeh et al., 2014).

Today there are several techniques being investigated for  $\text{CO}_2$  separation from post-combustion flue gas: absorption, adsorption, cryogenic distillation and membrane separation, where absorption is largely implemented today (Songolzadeh et al., 2014). In the absorption process, flue gas containing  $\text{CO}_2$  is cooled and dissolved in a solvent. The solvent reacts with the  $\text{CO}_2$  forming a weakly bonded intermediate compound thus absorbing the  $\text{CO}_2$ . For  $\text{CO}_2$  separation the solution is heated and stripped of the  $\text{CO}_2$  regenerating the absorbent solution and is further cooled for reuse (M. Wang et al., 2011).

In this work we look at swing adsorption technologies that use pressure/vacuum or temperature for adsorption/desorption cycles to separate  $\text{CO}_2$  from flue gas. These adsorption-based technologies are pressure/vacuum swing adsorption (PSA/VSA) and temperature swing adsorption (TSA). With the difference being the strategy for regeneration of the adsorbent. A swing adsorption process could reduce the energy and cost required for the separation of  $\text{CO}_2$  in post-combustion capture (Songolzadeh et al., 2014). Emissions from industries and power plants have different  $\text{CO}_2$  concentrations depending on the fuel. A coal burning power plants flue gas contains 12-15 vol.%  $\text{CO}_2$

and the exhaust steam from the production of iron and steel (blast furnace) consists of 20-44 vol.% CO<sub>2</sub> (Songolzadeh et al., 2014). These are point sources where an adsorption-based process could capture the CO<sub>2</sub> before it is emitted to the atmosphere and will be the focus of this work.

## **1.4. MECHANISMS OF ADSORPTION**

There are two main mechanisms of adsorption in terms of gas phase adsorption, chemisorption and physisorption. The categorization depends in practice on the binding energy of the adsorbed atom/molecule. Adsorption is a physical process that attaches an atom/molecule to a solid surface (M. Wang et al., 2011). This adsorption can be chemical, creating a bond, or physical and stay on the surface by weak Van der Waal forces or dipoles (Songolzadeh et al., 2014).

### **1.4.1. Chemisorption**

Chemisorption is when a chemical bond is formed between atoms/molecules or an exposed reaction surface, thus changing the electronic structure and forming covalent or ionic bonds (Songolzadeh et al., 2014). Forming this bond has an energy requirement that can be obtained by heat and the resulting molecule is thermodynamically stable. Such a process could be the formation of MgCO<sub>3</sub> from MgO and CO<sub>2</sub> (Xiao et al., 2011).

### **1.4.2. Physisorption**

Physisorption is the attachment of atoms/molecules on a solid surface that is mainly caused by the interaction of Van der Waal force (Karplus and Kolker, 1964). Other interactions include intermolecular and dipole forces. It can be a weak adsorption of gas molecules on a surface and the process barely disturb the electronic structure or the molecule of the sorbent surface (Songolzadeh et al., 2014). The process is temperature sensitive because of the weak interacting forces and can generally only be seen in environments of low temperature (Xiao et al., 2011).

## **1.5. SWING ADSORPTION**

Swing adsorption methods can use temperature or pressure differences to swing from an adsorbed to a desorbed state of atoms/molecules on a reaction surface, thereby regenerating a material (M. Wang et al., 2011). Swing adsorption in carbon capture is often TSA or PSA/VSA and is used to adsorb and desorb CO<sub>2</sub> from reaction surfaces (M. Wang et al., 2011). The difference between these technologies is based on the strategy for regeneration of an adsorbent after the adsorption process (Songolzadeh et al., 2014).

### **1.5.1. Temperature swing adsorption (TSA)**

TSA shifts between temperatures to desorb molecules that have been adsorbed to a surface. This can regenerate an adsorption material for further use. With this process, when CO<sub>2</sub> is to be separated from a sorbent for storage, heat from flue gas can be used for that desorption, eliminating a potentially costly heating process (Xiao et al., 2011).

In a coal burning powerplant, the gas exiting the gasifier after cleanup is typically at 400 °C, entering the gas turbine at around 250 °C where it can adsorb to magnesium-based materials, usually with a CO<sub>2</sub> content of about 15 vol.% and 85 vol.% N<sub>2</sub> (Songolzadeh et al., 2014; Xiao et al., 2011). At the gasifier temperature of 400 °C, magnesium-based materials have a potential to desorb CO<sub>2</sub> and regenerate (S. Wang et al., 2011).

In a blast furnace, exhaust steam containing CO<sub>2</sub> (20-44 vol.%) usually enters a carbonator at around 650 °C where the CO<sub>2</sub> can get reacted with lime (CaO) and form CaCO<sub>3</sub> in an exothermic reaction (Songolzadeh et al., 2014; S. Wang et al., 2011). The CaCO<sub>3</sub> can then be transferred to the calciner where the temperature is around 800-900 °C (Hilz et al., 2018). At these high temperatures calcium-based materials have a potential to desorb CO<sub>2</sub> and regenerate (S. Wang et al., 2011). When CO<sub>2</sub> gets separated from the bound solid phase of the sorbent, it is an endothermic reaction and the CO<sub>2</sub> can leave the calciner with the CaO regenerated and recycled (Hilz et al., 2018).

TSA are associated to difficulties with the thermal durability of sorption materials, degenerating the sorbent each cycle due to sintering and the formation of large single crystals (S. Wang et al., 2011). However, TSA is in carbon capture in conjunction with relatively high adsorption capacities (S. Wang et al., 2011).

### **1.5.2. Pressure/Vacuum swing adsorption (PSA/VSA)**

PSA/VSA can use pressure differences to swing between an adsorbed and desorbed state of atoms/molecules on a solid reaction surface (Webley et al., 2017). The process is thermally sensitive and operates under low, often ambient temperatures. The attachment of atoms/molecules on a solid surface is mainly caused by the interaction of Van der Waals force in addition to intermolecular and dipole forces (Karplus and Kolker, 1964; S. Wang et al., 2011). This adsorption process can also adsorb other atoms/molecules such as N<sub>2</sub> with flue gas consisting of up to 85 vol.%. Another process, when upgrading raw biogas with typically 40 vol.% CO<sub>2</sub> including impurities, CO<sub>2</sub> is separated from methane (CH<sub>4</sub>) that can also adsorb to reaction surfaces (Bacsik et al., 2016). This makes the CO<sub>2</sub> selectivity of an adsorbent important to be desirable for CO<sub>2</sub> separation in carbon capture (S. Wang et al., 2011).

The biggest physical adsorbents suggested for CO<sub>2</sub> adsorption include activated carbons, silicates and zeolites (Songolzadeh et al., 2014). The weak interaction and adsorption of CO<sub>2</sub> gas molecules on a reaction surface barely disturb the electronic structure or the molecule of the sorbent which minimizes sintering in this process (Songolzadeh et al., 2014). However, for every adsorption-desorption cycle with pressure differences, CO<sub>2</sub> can remain on the surface and in the pores of porous materials causing a degeneration each desorption cycle (Songolzadeh et al., 2014). Adsorption materials can however be heat-regenerated under low temperatures (Bacsik et al., 2016).

## **1.6. ADSORBENT MATERIALS**

In general, when considering suitable sorption materials for efficient CO<sub>2</sub> capture, the materials must have high CO<sub>2</sub> selectivity, high adsorption capacity, favorable operation temperature, fast adsorption/desorption kinetics and possess good thermal and mechanical cyclic stability (Songolzadeh et al., 2014; S. Wang et al., 2011). CO<sub>2</sub> is an acidic gas that is considered to adsorb on the basic sites of some metal oxides (Songolzadeh et al., 2014; S. Wang et al., 2011). Particularly metal oxides (MgO, CaO) with lower charge per radius ratio possessing a more ionic nature and thereby stronger basic sites (S. Wang et al., 2011).

Conventional solid CO<sub>2</sub> adsorbents are classified into three temperature ranges, low (below 200 °C), intermediate (200-400 °C) and high (above 400 °C) (S. Wang et al., 2011).

### 1.6.1. Low temperature sorbents

Activated carbon, zeolite, alumina, metal organic framework (MOF), alkali metal carbonates and amines are typically classified to the low temperature range (0-200 °C) and are relatively effective in physisorption (Songolzadeh et al., 2014; S. Wang et al., 2011). Synthesized mesoporous magnesium carbonate in this work showed 1.52 mmol g<sup>-1</sup> uptake at 0 °C (Table 7).

### 1.6.2. Intermediate temperature sorbents

Hydrotalcite-like compounds (HTlcs) and magnesium based materials e.g. MgO is considered to have an optimal CO<sub>2</sub> adsorption and desorption in the intermediate range (200-400 °C), which is useful for chemisorption (S. Wang et al., 2011). Purchased hydrotalcite tested as a reference in this work showed an uptake of 0.58 mmol g<sup>-1</sup> at 200 °C (Table 4).

### 1.6.3. High temperature sorbents

Calcium based materials (e.g. CaO), Li<sub>2</sub>ZrO<sub>3</sub> and Li<sub>4</sub>SiO<sub>4</sub> have been developed by the engineering and scientific community to selectively and reversibly act as CO<sub>2</sub> sorbents at elevated temperatures (above 400 °C) (Songolzadeh et al., 2014; S. Wang et al., 2011; Xiao et al., 2011). Mesoporous calcium carbonate that was synthesized in this work showed an uptake of 14.96 mmol g<sup>-1</sup> at 650 °C (Table 4).

## 1.7. MESOPOROUS INORGANIC CARBONATES (MIC)

Nanoporous materials are constituted by microporous (avg. pore size < 2 nm) and mesoporous (avg. pore size ~2-50 nm) materials, with probably the most well-known being the zeolites (< 2 nm) (Cheung et al., 2016). The small pore size of zeolites can be desirable for applications with small molecules. However, different types of mesoporous materials have been well studied for applications involving larger molecules (Cheung et al., 2016; S. Wang et al., 2011). These include activated carbon, alumina, mesoporous silica and alkali metal carbonates (S. Wang et al., 2011). Of these, mesoporous inorganic carbonates (MIC) are the most studied (Cheung et al., 2016). A useful aspect of some mesoporous materials is the ability to tailor the pore size for applicational use. Methods of controlling the pore size include surfactants and temperature control during synthesis (Forsgren et al., 2013).

MMC was first reported in 2013 with the synthesis documented elsewhere (Forsgren et al., 2013), and summarized in this work (2.2.1 MMC). MMC is a stable amorphous nanostructure partly consisting of aggregated nanometer sized MgO crystals that is synthesized at low temperature. The resulting material is coated with amorphous MgCO<sub>3</sub> (Figure 1, right) and is aggregated together with nanocrystals adhered by MgCO<sub>3</sub> throughout the material structure (Cheung et al., 2016). MMC has a unique porous structure within a 6 nm size range and an exceptionally high surface area (800 m<sup>2</sup> g<sup>-1</sup>) (Forsgren et al., 2013). The weight percentage characteristics of MMC is about ~15 wt.% MgO and ~85 wt.% MgCO<sub>3</sub> (Cheung et al., 2016).

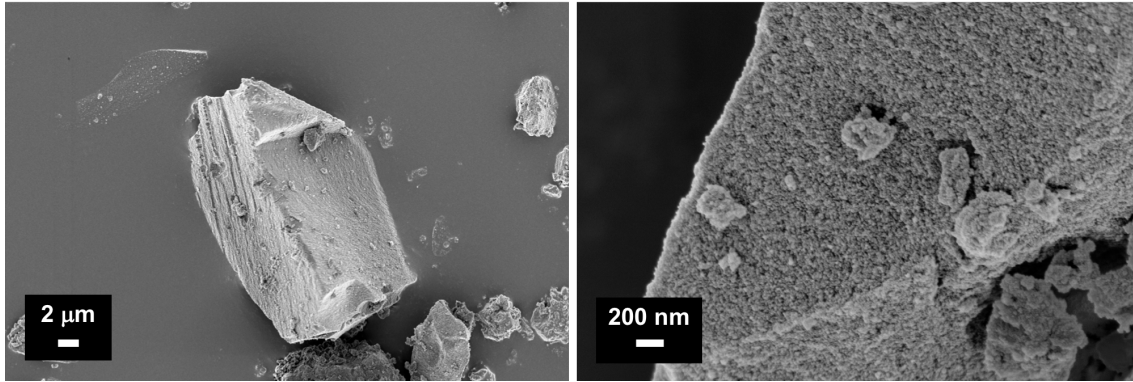


**Figure 1.** Scanning electron microscope micrographs of MMC. Bracket size magnification reference left 2  $\mu\text{m}$ , right 200 nm.

MCC is made in a similar process as MMC but with CaO as a base material. MCC is mesoporous with amorphous, aggregated nanometer sized CaO crystals throughout the structure (unpublished results).

MCMC is a combined structure material synthesized by different ratios of CaO/MgO in a similar process as MMC with an amorphous and mesoporous structure (unpublished results).

## 2. MATERIALS AND METHODS

### 2.1. MATERIALS

#### 2.1.1. Base materials

Three base materials were tested and further combined with additives to increase CO<sub>2</sub> capture characteristics in this work. All three materials are mesoporous inorganic carbonates (MIC) and include mesoporous magnesium carbonate (MMC), mesoporous calcium carbonate (MCC) and a combined structure material of mesoporous calcium magnesium carbonate (MCMC). MIC was in this work tested with additives based on different weight percentages of CaO, Al(NO<sub>3</sub>)<sub>3</sub>, Al<sub>2</sub>O<sub>3</sub>, K<sub>2</sub>CO<sub>3</sub> and KNO<sub>3</sub> (Table 1) that were introduced into the porous structure during synthesis.

**Table 1.** Materials used in this work, manufacturer and content purity.

Materials	Manufacturer	Purity
Magnesium carbonate (MgCO <sub>3</sub> )	Sigma-Aldrich, Japan	R&D grade ≥99% trace metals basis
Magnesium oxide (MgO)	Sigma-Aldrich, USA	
Calcium carbonate (CaCO <sub>3</sub> )	Sigma-Aldrich, Japan	≥99.0% Reagent grade, Trace metals
Calcium oxide (CaO)	Alfa Aesar, Germany	0.01% max Puriss. p.a.
Aluminum nitrate (Al(NO <sub>3</sub> ) <sub>3</sub> × 9H <sub>2</sub> O)	Sigma-Aldrich, USA	≥98.0% (KT) R&D grade nanopowder.
Aluminum oxide (Al <sub>2</sub> O <sub>3</sub> )	Sigma-Aldrich, Germany	<50 nm Puriss. p.a.
Potassium carbonate (K <sub>2</sub> CO <sub>3</sub> )	Sigma-Aldrich, USA	≥99.0% (T)
Potassium nitrate (KNO <sub>3</sub> )	Alfa Aesar, Germany	99.0% minimum

#### 2.1.2. Reference materials

In order to justify synthesizing mesoporous materials (MMC, MCC, MCMC) and trying to improve them with additives, the purchased stock materials (MgCO<sub>3</sub>, MgO, CaCO<sub>3</sub>, CaO) were used as references and tested in their pure form. The well-studied conventional material hydrotalcite was also purchased and used as a reference. The reference materials performance in CO<sub>2</sub> uptake and thermal stability was put in comparison to the synthesized MIC and additives.

#### 2.1.3. Additives – Thermal stability and sintering

Additives combined with the base materials were thought to solve the sintering problem inherent to magnesium and calcium-based sorbents under heat regeneration, by being distributed uniformly among the crystallites, acting like frameworks in the porous

structures. Thereby inhibiting the sintering and formation of large (MgO, CaO) single crystals during multiple adsorption-desorption cycles (S. Wang et al., 2011).

Potassium-based additives ( $K_2CO_3$  and  $KNO_3$ ) were chosen due to previous studies showing promising effects on increasing the  $CO_2$  uptake on hydrotalcites at moderate temperatures (Walspurger et al., 2008). The additives were further theorized to likewise act as frameworks.

MCMC as a binary material was thought to alleviate the sintering problem of the sole MCC molecule each adsorption-desorption cycle, due to the magnesium acting as an inert material and a supporting framework to the calcium. This is due to the magnesium not readily adsorbing  $CO_2$  under the high operation temperatures (above  $400\text{ }^\circ\text{C}$ ) (S. Wang et al., 2011). This could improve the thermal stability of the sorbent while still maintaining a high adsorption capacity. When calcium-based  $CO_2$  sorbents is regenerated at high temperatures ( $850\text{ }^\circ\text{C}$ ), CaO sintering results in the decrease of specific surface area and porosity, which are important for the reaction with  $CO_2$  (Li et al., 2006).

Aluminum-based additives ( $Al_2O_3$  and  $Al(NO_3)_3$ ) were chosen due to their strong affinity for  $CO_2$  adsorption (Chen and Ahn, 2011) and to reproduce the chemical compositions of the well-studied Mg/Al based  $CO_2$  adsorbent hydrotalcite, which has advantageous characteristics such as fast kinetics, high adsorption capacity, thermal cyclic stability and is easy to prepare compared to other HTIcs (Bhatta et al., 2015). Aluminum was thought to improve the combined structure of MCMC by inhibiting sintering to a greater extent.

## **2.2. SYNTHESIS**

### **2.2.1. Mesoporous magnesium carbonate (MMC)**

In summary, MMC consist of a stable amorphous nanostructure synthesized at room temperature by homogeneously dispersing 20 g of MgO (Sigma-Aldrich, USA) in 300 ml methanol (VWR, Sweden) with stirring in a reinforced glass pressure reaction vessel ( $350\text{ cm}^3$ ) purchased from Andrew Glass Co., USA. The mixture was then pressurized with 4 bar of  $CO_2$  and sealed for 24 hours under stirring. Afterwards, the  $CO_2$  pressure inside the reaction vessel was released and a cloudy solution was obtained. The solution was centrifuged at 3800 rpm for 30 minutes to obtain a clear, yellow colored liquid. The separated solid particles were discarded. Gelation of the clear yellow colloidal suspension was induced by mechanical stirring under heat ( $55\text{ }^\circ\text{C}$ ) in a ventilated fume hood. The reaction mixture thickened into an alcogel before breaking up into small, wet powder-like pieces. The pieces was dried into a powder by heating at  $150\text{ }^\circ\text{C}$  for 24 hours (Cheung et al., 2016).

### **2.2.2. Mesoporous calcium carbonate (MCC)**

MCC was synthesized with a similar procedure as MMC but with calcium oxide homogeneously dispersed in methanol. The clear liquid was dried into a powder by heating in an oven for 3 hours.

### **2.2.3. Mesoporous calcium magnesium carbonate (MCMC)**

This combined material was synthesized with methods closely resembling MMC but using ratios of calcium oxide and magnesium oxide homogeneously dispersed in methanol. The clear liquid was dried into a powder by heating it in an oven for 24 hours. For different ratios, the materials added ( $CaO$ ;  $M = 56.077\text{ g mol}^{-1}$ ,  $MgO$ ;  $M = 40.304\text{ g mol}^{-1}$ ) are calculated by their molar mass to obtain a desired ratio.

#### **2.2.4. Mesoporous magnesium carbonate (MMC) with additives**

Four different materials (Table 1,  $\text{Al}(\text{NO}_3)_3$ ,  $\text{Al}_2\text{O}_3$ ,  $\text{K}_2\text{CO}_3$ ,  $\text{KNO}_3$ ) were introduced into the porous structure of MMC as additives. The synthesis of MMC with additives was carried out in a similar manner as described above. After the centrifuge step, different amounts of additives were added to the gelation reaction mixture before the colloidal suspension was induced by mechanical stirring. Therefore, the same procedures as for the synthesis of MMC was adopted.

#### **2.2.5. Mesoporous calcium magnesium carbonate (MCMC) with additives**

The synthesis of MCMC with additives was made similarly to the MMC synthesis. Different amounts of additives (Table 1,  $\text{Al}(\text{NO}_3)_3$ ,  $\text{K}_2\text{CO}_3$ ) were added to the reaction mixture together with MgO and CaO in methanol at the beginning of the synthesis. Further, the same procedures as for the synthesis of MMC was performed.

### **2.3. ANALYTICAL TECHNIQUES FOR CHARACTERIZATION**

#### **2.3.1. Powder X-ray diffraction (XRD)**

XRD analysis was performed using a Bruker D8 Advanced XRD Twin Twin diffractometer unit (Billerica, Massachusetts, USA). The unit used  $\text{Cu-K}\alpha$  radiation with wavelength 1.54 Å for  $2\theta = 10.0\text{-}90.0^\circ$  at room temperature. Samples were ground and administered with pure ethanol on a silicon sample holder with zero background prior to analysis. The instrument was set to operate at 45 kV and 40 mA.

Powder X-ray diffraction provides information about crystalline phases and specific lattices of powdered materials which diffracts x-rays on crystallographic planes. The lattice parameters make the x-rays diffract to form specific peaks. When an amorphous material is examined using XRD an x-ray amorphous peak can be seen, as seen in Figure 4 to Figure 6 (left).

#### **2.3.2. Volumetric gas adsorption (BET)**

Surface area was determined by Brunauer-Emmett-Teller (Brunauer et al., 1938), by performing nitrogen adsorption and desorption isotherms at  $-195^\circ\text{C}$  using a Micromeritics Accelerated Surface Area and Porosimetry (ASAP) 2020 analyzer (Norcross, GA, USA). Data points from the equilibrium adsorption were recorded when the pressure change dropped below 0.01 % during 10 s intervals with a minimum 100 s delay. Samples were heated ( $100^\circ\text{C}$ ) under dynamic vacuum ( $1 \cdot 10^4 \text{ Pa}$ ) prior to analysis, using a Micromeritics SmartVacPrep sample preparation unit. Analyzing the nitrogen sorption isotherms give information about the pore size distribution and surface area of samples.

#### **2.3.3. Scanning electron microscope (SEM)**

Micrographs of materials were made with a SEM. The units used were Zeiss LEO 1530 and 1550 instruments, equipped with in-lens detectors and operating at 2 kV. Samples were ground and put on a stub holder with double-sided carbon tape. The stub holder with sample were further sputter coated with a thin layer of gold/palladium prior to analysis. With a large depth of focus, the SEM is a powerful tool to visualize the surface of a sample and can provide an intuitive picture of a material.

## 2.4. CARBON CAPTURE TECHNIQUES

### 2.4.1. Temperature swing adsorption (TSA)

TSA was carried out using a thermogravimetric analysis (TGA) Mettler Toledo TGA 2 instrument with sample sizes of approximately 40 mg. TGA analysis records the change of a samples mass under controlled heating and gives information about the bonding strength and decomposition of the molecules in the sample.

Temperature for CO<sub>2</sub> desorption (calcination) was 450 °C and CO<sub>2</sub> adsorption (carbonation) 200 °C, used for magnesium-based materials, chosen due to typical flue gas exiting a gasifier (450 °C) and gas turbine (200 °C) of coal burning power plants (Xiao et al., 2011). The high calcination temperature 850 °C and CO<sub>2</sub> adsorption 650 °C, used for calcium-based materials, was chosen due to typical exhaust steam in the calciner (850 °C) and carbonator (650 °C) of blast furnace industries (Hilz et al., 2018).

Samples were heated under 50 ml min<sup>-1</sup> N<sub>2</sub> flow from room temperature in an inert alumina cup to the material specific calcination temperature with the heating rate 10 °C min<sup>-1</sup>. This was followed by a temperature decrease of 10 °C min<sup>-1</sup> to the material specific CO<sub>2</sub> capture temperature. This temperature was held under a 50 ml min<sup>-1</sup> CO<sub>2</sub> flow adsorbing to the sample. The sample was reheated to the material specific calcination temperature under N<sub>2</sub> flow, followed by three cycles of CO<sub>2</sub> adsorption and desorption. The best performing samples were subjected to 23 cycles of CO<sub>2</sub> adsorption and desorption to test the long-term effects on the materials.

In the example in Figure 2, CO<sub>2</sub> adsorbs to the sample at the carbonation temperature 250 °C, at time 0 s. At time 3600 s the calcination temperature 450 °C is applied and the CO<sub>2</sub> is desorbed from the sample. This is repeated for cyclic measurements. The same method is used for the carbonation temperature 650 °C and the calcination temperature 850 °C. Note that in Figure 2, the top at 3600 s is an anomaly produced by the TGA instrument.

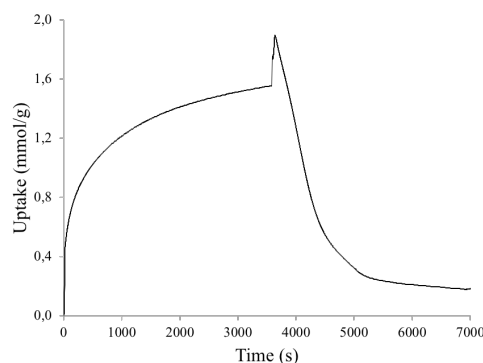


**Figure 2.** One cycle of adsorption and desorption of CO<sub>2</sub> using TSA.

### 2.4.2. Vacuum swing adsorption (VSA)

VSA of CO<sub>2</sub> and N<sub>2</sub> was performed using a Micromeritics ASAP 2020 surface area analyzer (Norcross, GA, USA). Samples were prepared in a glass measurement tube with an average sample weight of 150 mg. Samples were heated to 100 °C under dynamic vacuum ( $1 \cdot 10^4$  Pa) in the glass tube prior to analysis, using a Micromeritics SmartVacPrep sample preparation unit. The adsorption of CO<sub>2</sub> and N<sub>2</sub> was performed at 0 °C from 0 to 101 kPa (1 atm). The measurement tube was evacuated and submerged in a vessel filled with ice water (0 °C) and a flow of a hypothetical flue gas was applied inside the tube, considered to contain 15 vol.% CO<sub>2</sub> and 85 vol.% N<sub>2</sub>. CO<sub>2</sub> and N<sub>2</sub>

adsorption isotherms at 0 °C were recorded. Further, the tube was evacuated and desorption isotherms at 0 °C were recorded. Due to time constraints this experiment was performed for one cycle for each sample. The best performing samples were subjected to further cyclic experiments.

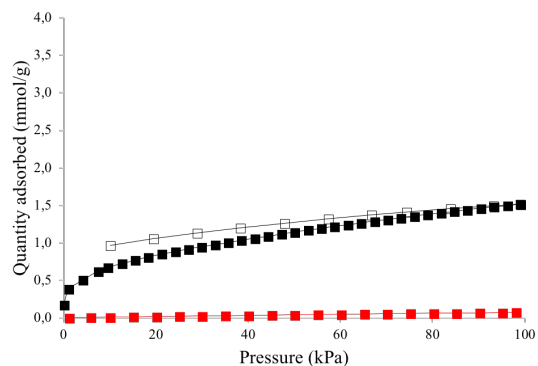


**Figure 3.** One cycle of CO<sub>2</sub> adsorption (black solid squares), desorption (hollow squares) and N<sub>2</sub> adsorption (red solid squares).

### 3. RESULTS AND DISCUSSION

#### 3.1. CHARACTERIZATION

##### 3.1.1. Morphology and structure

MMC synthesized in this work had a nanostructure consisting of nanometer sized MgO crystals aggregated together with nanocrystals of MgCO<sub>3</sub> yielding a high porosity. The porosity of MMC being the space between nanoparticles, confirmed to be present with BET (Table 2) and SEM (Figure 4, right) as the rough dimpled surface. Note that the size of nanoparticles shown in SEM micrographs is not representative due to sample coating of gold/palladium nanoparticles. The pores of MMC was around 4 nm on average, while the total pore volume was around 0.54 cm<sup>3</sup> g<sup>-1</sup>, concluded from BET analysis, prior to gold/palladium coating. Further, the small nanoparticles also meant that MMC was X-ray amorphous. This is shown in the powder XRD pattern in Figure 4 (left), where the pattern contains no crystalline diffraction peaks.

As synthesized MCC (Figure 5, right) and MCMC (Figure 6, right) was with SEM shown to have aggregated nanometer sized particles throughout the structure and being X-ray amorphous as seen in XRD patterns in Figure 5 and Figure 6 (left).

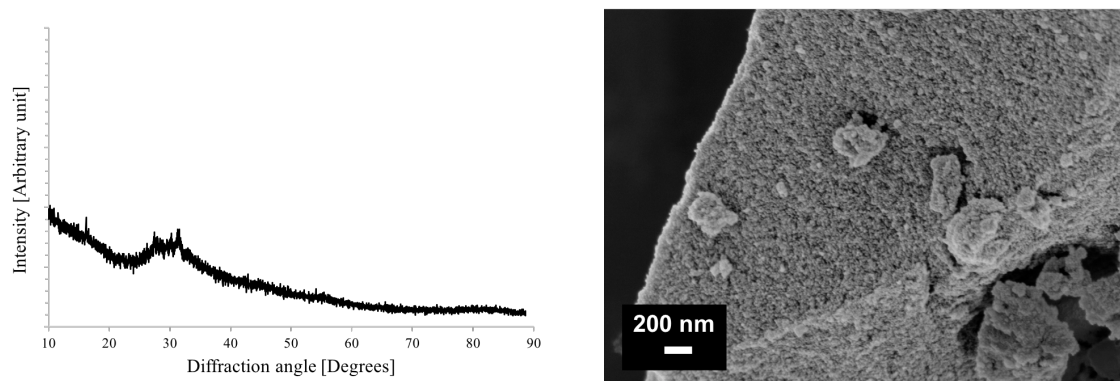


**Figure 4.** Powder X-ray diffraction (left) and SEM micrograph (right) of as synthesized MMC.

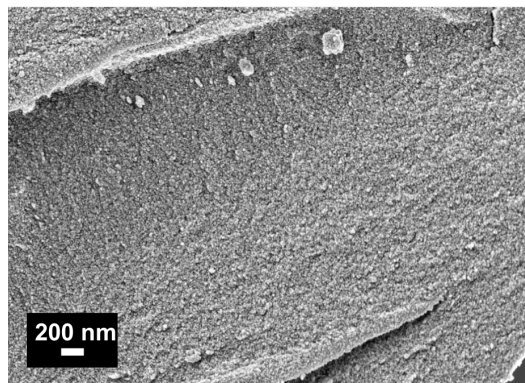
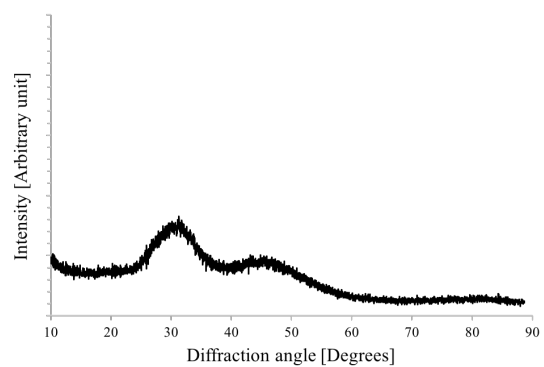


**Figure 5.** Powder X-ray diffraction (left) and SEM micrograph (right) of as synthesized MCC.

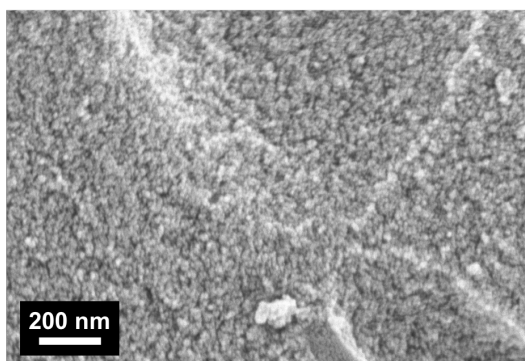
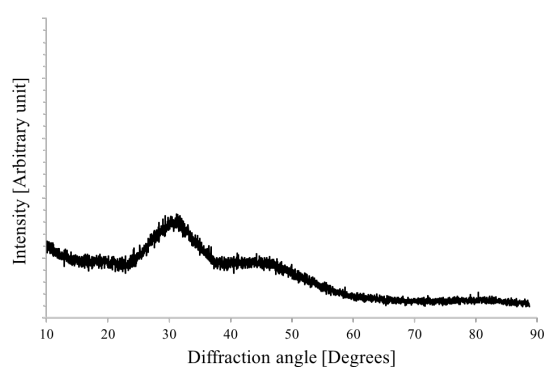


**Figure 6.** Powder X-ray diffraction (left) and SEM micrograph (right) of as synthesized MCMC with calcium and magnesium in the ratio 3:1.

The specific surface area of the base materials was characterized by N<sub>2</sub> adsorption/desorption isotherms (2.3.2 Volumetric gas adsorption) and are presented in Table 2, in relation to reference materials. The synthesized base materials in this work are shown to largely have a higher BET specific surface area compared to purchased, unmodified materials. This is due to the synthesis of the materials, which is developed to leave behind pores during the evaporation of methanol (2.2 Synthesis).

**Table 2.** Base\* and reference materials with BET surface area.

Sample name	BET surface area (m <sup>2</sup> g <sup>-1</sup> )
MMC*	698
MCC*	394
MCMC (Ca/Mg) 3:1*	490
Sigma-Aldrich Synthetic Hydrotalcite	10
Sigma-Aldrich MgCO <sub>3</sub>	20
Sigma-Aldrich MgO	120
Sigma-Aldrich CaCO <sub>3</sub>	1
Alfa Aesar CaO	3

### 3.1.2. Additive characterization

MCMC were synthesized with different ratios of CaO/MgO (Table 3) to see changes in stability and uptake. MCMC 3:1 was chosen as a base material to be further combined with additives due to the materials relatively high initial uptake (13.32 mmol g<sup>-1</sup>, Table 4) with TSA (850-650 °C) and its relatively high thermal stability, with an uptake of 8.56 mmol g<sup>-1</sup> at the 23<sup>rd</sup> cycle (Figure 7). The uptake of MCMC 3:1 is relatively high due to the inherent capabilities of the calcium material in these temperature ranges and the stability is thought to be improved by the combination of magnesium which is inert at these temperatures and probably acts as a framework that mitigates sintering.

Additives introduced to the MCMC 3:1 material were 10 to 45 wt.% of Al(NO<sub>3</sub>)<sub>3</sub> and an addition of 25 wt.% K<sub>2</sub>CO<sub>3</sub>. Adding K<sub>2</sub>CO<sub>3</sub> to MCMC destroyed the structure leaving it with an initial uptake of 1.25 mmol g<sup>-1</sup> (Table 5, TSA, 850-650 °C) and no further experiments were made with MCMC 3:1 K 25 wt.%. Adding various weight percentages of Al(NO<sub>3</sub>)<sub>3</sub> to MCMC 3:1 lowered the BET surface area with higher additive percentages (Table 3). However, higher additive percentages of Al increased the thermal stability of MCMC while maintaining a high uptake of around 13 mmol g<sup>-1</sup> (Figure 7). This extended up to an addition of 45 wt.% Al, where the uptake was drastically halved (Table 5), and no further experiments were made with MCMC 3:1 Al 45 wt.%.

Additives introduced to the MMC material were various weight percentages of Al(NO<sub>3</sub>)<sub>3</sub>, Al<sub>2</sub>O<sub>3</sub>, K<sub>2</sub>CO<sub>3</sub> and KNO<sub>3</sub> causing a marginally lowered BET surface area (Table 3) compared to as synthesized MMC (698 m<sup>2</sup> g<sup>-1</sup>, Table 2). However, the addition of 5 wt.% K<sub>2</sub>CO<sub>3</sub> (for MMC-K<sub>2</sub>CO<sub>3</sub> 5 wt.%) as much as doubled the uptake

(3.24 mmol g<sup>-1</sup>) using VSA (at 101 kPa, 0 °C) compared to MMC (1.52 mmol g<sup>-1</sup>) under the same conditions (Table 7). The uptake was greatly increased for MMC-Al<sub>2</sub>O<sub>3</sub> 10 wt.% (2.68 mmol g<sup>-1</sup>) and MMC-KNO<sub>3</sub> 5 wt.% (2.49 mmol g<sup>-1</sup>). Though, marginally for MMC-Al(NO<sub>3</sub>)<sub>3</sub> 10 wt.% (1.90 mmol g<sup>-1</sup>). Depicted in Table 3 are all the additives with changes to BET surface area.

**Table 3.** Amount of additives on MMC and MCMC with BET surface area.

Sample name	Additive and amount	BET surface area (m <sup>2</sup> g <sup>-1</sup> )
MMC-Al(NO <sub>3</sub> ) <sub>3</sub> 10 wt.%	Al(NO <sub>3</sub> ) <sub>3</sub> · 9H <sub>2</sub> O, 10 wt.%	518
MMC-Al <sub>2</sub> O <sub>3</sub> 10 wt.%	Al <sub>2</sub> O <sub>3</sub> , 10 wt.%	580
MMC-K <sub>2</sub> CO <sub>3</sub> 15 wt.%	K <sub>2</sub> CO <sub>3</sub> , 15 wt.%	490
MMC-K <sub>2</sub> CO <sub>3</sub> 10 wt.%	K <sub>2</sub> CO <sub>3</sub> , 10 wt.%	599
MMC-K <sub>2</sub> CO <sub>3</sub> 5 wt.%	K <sub>2</sub> CO <sub>3</sub> , 5 wt.%	637
MMC-KNO <sub>3</sub> 10 wt.%	KNO <sub>3</sub> , 10 wt.%	499
MMC-KNO <sub>3</sub> 5 wt.%	KNO <sub>3</sub> , 5 wt.%	563
MCMC 1:3	CaO/MgO, 1:3	623
MCMC 1:2	CaO/MgO, 1:2	539
MCMC 1:1	CaO/MgO, 1:1	543
MCMC 2:1	CaO/MgO, 2:1	572
MCMC 3:1	CaO/MgO, 3:1	490
MCMC 3:1 Al 45 wt.%	3:1, Al(NO <sub>3</sub> ) <sub>3</sub> · 9H <sub>2</sub> O, 45 wt.%	[-]
MCMC 3:1 Al 35 wt.%	3:1, Al(NO <sub>3</sub> ) <sub>3</sub> · 9H <sub>2</sub> O, 35 wt.%	306
MCMC 3:1 Al 25 wt.%	3:1, Al(NO <sub>3</sub> ) <sub>3</sub> · 9H <sub>2</sub> O, 25 wt.%	418
MCMC 3:1 Al 10 wt.%	3:1, Al(NO <sub>3</sub> ) <sub>3</sub> · 9H <sub>2</sub> O, 10 wt.%	501
MCMC 3:1 K 25 wt.%	3:1, K <sub>2</sub> CO <sub>3</sub> , 25 wt.%	[-]

### 3.2. CO<sub>2</sub> TEMPERATURE SWING ADSORPTION

In this section TSA was used to test samples for CO<sub>2</sub> adsorption capacity, cyclic stability and uptake kinetics in the industry favorable temperature ranges 200-450 °C and 650-850 °C. Samples were heated from room temperature to the calcination temperature,

followed by a temperature decrease to the sorption temperature. This was repeated for three cyclic measurements for all samples with further intensive testing for the best samples.

### 3.2.1. CO<sub>2</sub> adsorption capacity - References

The CO<sub>2</sub> uptake of as synthesized MMC reached around 1.46 mmol g<sup>-1</sup> (in the 200 to 450 °C temperature range), which is marginally lower than the CO<sub>2</sub> uptake of purchased, unmodified MgCO<sub>3</sub> (1.51 mmol g<sup>-1</sup>, Table 4). However, higher than purchased synthetic hydrotalcite (0.58 mmol g<sup>-1</sup>), making MMC a candidate for further addition of additives.

MCC has a relatively high CO<sub>2</sub> uptake (14.96 mmol g<sup>-1</sup>) in the 650-850 °C temperature range, which is drastically lowered due to sintering after continuous TSA cycles (Figure 7, left). The combined material MCMC 3:1, lowers the initial uptake by around 2 mmol g<sup>-1</sup> compared to MCC and is marginally higher than purchased CaCO<sub>3</sub>. However, the thermal and cyclic stability is greatly improved compared to purchased CaCO<sub>3</sub> (Figure 7, left). All base materials and reference materials initial TSA uptake of CO<sub>2</sub> with corresponding sorption and regeneration temperatures are presented in Table 4.

**Table 4.** Base and reference materials CO<sub>2</sub> uptake on the first cycle, using TSA.

Sample name	CO <sub>2</sub> uptake (mmol g <sup>-1</sup> )	Sorption T/°C	Regeneration T/°C
		200	450
MMC	1.46		
Hydrotalcite	0.58		
MgCO <sub>3</sub>	1.51		
MgO	0.30		
		650	850
MCC	14.96		
MCMC 3:1	13.32		
CaCO <sub>3</sub>	12.78		
CaO	1.47		

### 3.2.2. CO<sub>2</sub> adsorption capacity - Additives

None of the additives on MMC increased the initial CO<sub>2</sub> uptake with TSA in the 200-450 °C temperature range, probably due to the degeneration of the porous structure. MMC with additives was seen as better candidates for vacuum swing adsorption and in the case of MMC-K<sub>2</sub>CO<sub>3</sub> 5 wt.%, for adsorption at room temperature and low temperature regeneration (3.4 CO<sub>2</sub> cycling at RT, Figure 21).

The various ratios of MCMC (CaO/MgO) in Table 5 show that a higher ratio of CaO yields an increased CO<sub>2</sub> uptake, thought to be due to the calcium having a high CO<sub>2</sub>

uptake at this temperature range while magnesium is only needed to a limited extent to act as a framework for stability. The addition of  $\text{Al}(\text{NO}_3)_3$  to MCMC 3:1 show a slight decrease in  $\text{CO}_2$  uptake with higher weight percentages. However, up to and including Al 35 wt.%, the material has an increase in thermal and cyclic stability (Figure 7, right).

**Table 5.** First cycle  $\text{CO}_2$  uptake on base materials with additives, using TSA.

Sample name	$\text{CO}_2$ uptake ( $\text{mmol g}^{-1}$ )	Sorption T/ $^\circ\text{C}$	
		200	450
MMC- $\text{Al}_2\text{O}_3$ 10 wt.%	0.76		
MMC- $\text{K}_2\text{CO}_3$ 15 wt.%	1.25		
MMC- $\text{K}_2\text{CO}_3$ 10 wt.%	1.13		
MMC- $\text{K}_2\text{CO}_3$ 5 wt.%	1.14		
MMC- $\text{KNO}_3$ 10 wt.%	0.43		
MMC- $\text{KNO}_3$ 5 wt.%	0.49		
		650	850
MCMC 1:3	5.62		
MCMC 1:2	7.22		
MCMC 1:1	10.12		
MCMC 2:1	12.66		
MCMC 3:1	13.32		
MCMC 3:1 Al 45 wt.%	6.18		
MCMC 3:1 Al 35 wt.%	12.23		
MCMC 3:1 Al 25 wt.%	13.15		
MCMC 3:1 Al 10 wt.%	13.49		
MCMC 3:1 K 25 wt.%	1.25		

### 3.2.3. CO<sub>2</sub> temperature swing cycling

TSA cycling of CO<sub>2</sub> in the 650-850 °C temperature range, show base materials (CaCO<sub>3</sub>, MCC and MCMC 3:1) all having a relatively high initial CO<sub>2</sub> uptake of around 13-15 mmol g<sup>-1</sup> (Figure 7, left), but quickly break down due to sintering into larger crystals. Notably, the purchased CaCO<sub>3</sub> porous structure breaks down the fastest, with an uptake of 2.60 mmol g<sup>-1</sup> at the 23<sup>rd</sup> cycle (Table 6). MCMC 3:1 has a higher uptake at the 23<sup>rd</sup> cycle (8.56 mmol g<sup>-1</sup>) compared to MCC with an uptake of 7.29 mmol g<sup>-1</sup> (Table 6), which indicates that the combined structure of MCMC improves thermal and cyclic stability.

MCMC 3:1 Al 35 wt.% (Figure 7, right) can be seen to be the most stable in thermal and cyclic stability, with an initial CO<sub>2</sub> uptake of 12.23 mmol g<sup>-1</sup> and an uptake of 10.96 mmol g<sup>-1</sup> at the 23<sup>rd</sup> cycle (Table 6). This indicates a relatively low sintering compared to the base materials and other weight percentages of Al.

**Table 6.** CO<sub>2</sub> uptake of references and MCMC with aluminum additives, first and last cycles.

Sample name	1 <sup>st</sup> cycle	23 <sup>rd</sup> cycle	CO <sub>2</sub> uptake (mmol g <sup>-1</sup> )
MCMC 3:1	13.32	8.56	
MCC	14.96	7.29	
Sigma CaCO <sub>3</sub>	12.76	2.60	
MCMC 3:1 Al 45 wt.%	6.18	5.52	
MCMC 3:1 Al 35 wt.%	12.23	10.96	
MCMC 3:1 Al 25 wt.%	13.03	10.84	
MCMC 3:1 Al 10 wt.%	13.49	8.91	

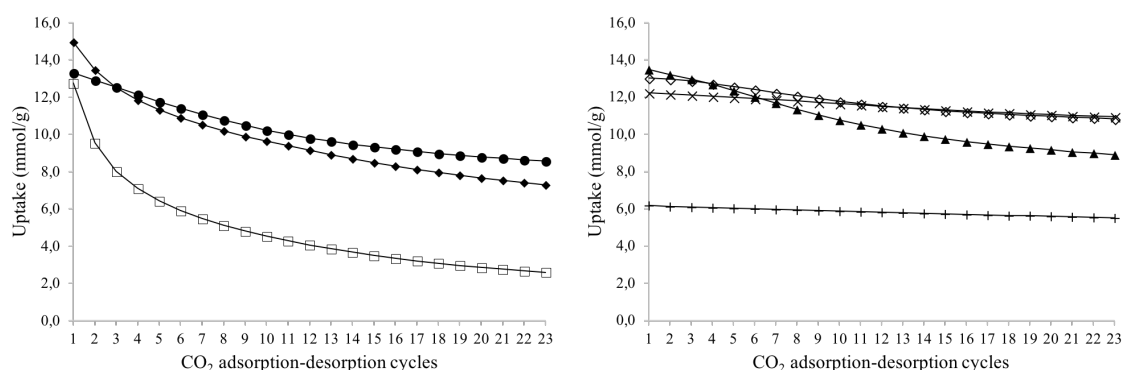


**Figure 7.** CO<sub>2</sub> adsorption-desorption for 23 cycles (850-650 °C). References, left; MCMC 3:1 (solid circles), MCC (solid diamonds) and Sigma CaCO<sub>3</sub> (hollow squares). Right; MCMC 3:1 Al 45 wt.% (pluses), Al 35 wt.% (crosses), Al 25 wt.% (hollow diamonds) and Al 10 wt.% (solid triangles).

### 3.2.4. Adsorption kinetics

Adsorption kinetics were observed with the CO<sub>2</sub> uptake at the first 100 seconds for samples using TSA. This was performed to see the effect of the additives introduced to the base materials in relation to the CO<sub>2</sub> capacity. As can be seen in Figure 8 to Figure 10 the first 100 seconds of a CO<sub>2</sub> adsorption-desorption cycle have been presented for the best performing samples. The most vertical curves and the curves most shifted to the left on the x-axis has the fastest adsorption kinetics.

MCMC 3:1 (Figure 8, left, green) is shown to marginally have the fastest CO<sub>2</sub> adsorption kinetics. Further, depicted in Figure 8 (right), an increase of aluminum indicates a deceleration of adsorption kinetics. This is probably due to the reduction of BET surface area after the implementation of additives, thus limiting the effect of the reaction surface.

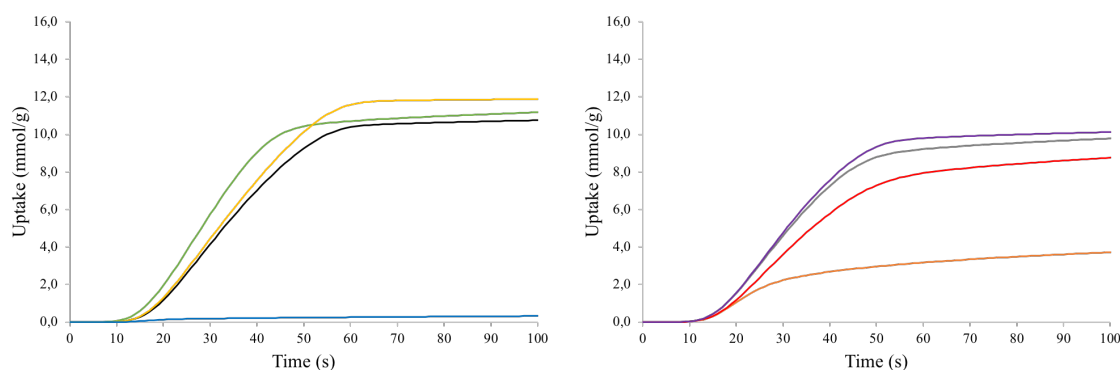


**Figure 8.** CO<sub>2</sub> adsorption kinetics, uptake at the first 100 seconds (650 °C). References, left; MCC (black), MCMC 3:1 (green), Sigma CaCO<sub>3</sub> (yellow) and Alfa aesar CaO (blue). Right; MCMC 3:1 Al 45 wt.% (orange), Al 35 wt.% (red), Al 25 wt.% (grey) and Al 10 wt.% (purple).

The base material MMC (Figure 9, left, black) is shown to have the fastest initial CO<sub>2</sub> adsorption kinetics compared to MMC with additives. The kinetics as seen in Figure 9 and Figure 10, indicates that an addition of additives decelerates the CO<sub>2</sub> uptake. The base material MMC is thought to have an unaltered porous structure, yielding a higher BET surface area, which lets CO<sub>2</sub> adsorption occur more extensively.

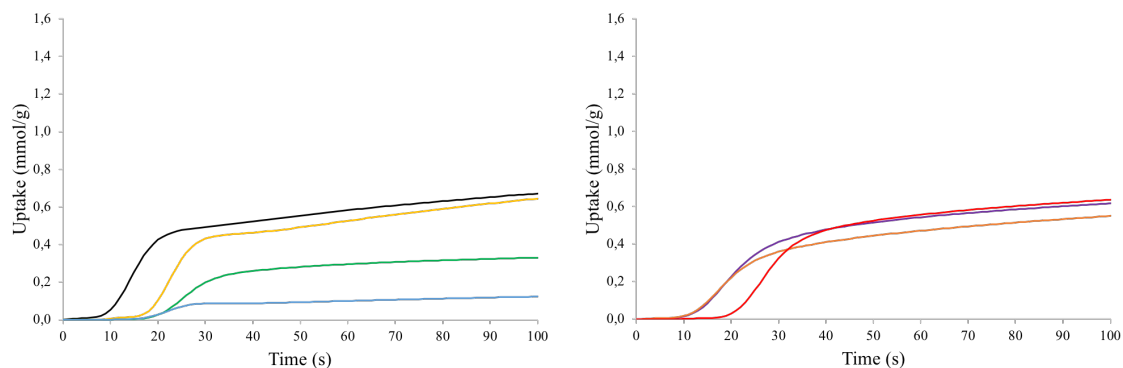


**Figure 9.** CO<sub>2</sub> adsorption kinetics, uptake at the first 100 seconds (200 °C). References, left; MMC (black), Synthetic hydrotalcite (green), Sigma MgCO<sub>3</sub> (yellow) and Sigma MgO (blue). Right; MMC-K<sub>2</sub>CO<sub>3</sub> 15 wt.% (purple), 10 wt.% (orange) and 5 wt.% (red).

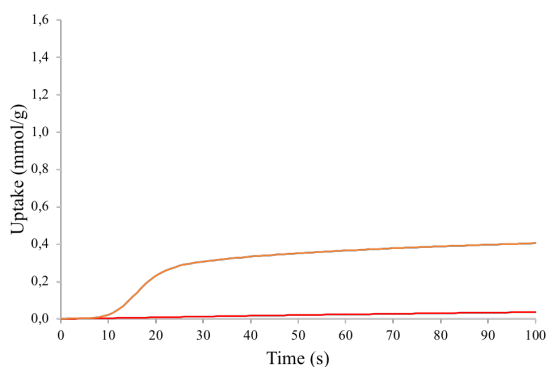


**Figure 10.** CO<sub>2</sub> adsorption kinetics, uptake at the first 100 seconds (200 °C) kinetics, (orange) MMC-Al<sub>2</sub>O<sub>3</sub> 10 wt.% and (red) MMC-Al(NO<sub>3</sub>)<sub>3</sub> 10 wt.%.

### 3.3. CO<sub>2</sub> VACUUM SWING ADSORPTION

In this section VSA was used to record CO<sub>2</sub> adsorption isotherms at 0 °C from 0 to 101 kPa, to determine the samples uptake capacity. For the best samples, this was repeated for cyclic measurements. N<sub>2</sub> adsorption isotherms was also recorded to determine selectivity in relation to CO<sub>2</sub>.

#### 3.3.1. CO<sub>2</sub> adsorption isotherms - References

As seen in Figure 11 to Figure 13, MMC show significantly higher CO<sub>2</sub> uptake than purchased MgCO<sub>3</sub>, MgO, CaCO<sub>3</sub>, CaO and hydrotalcite across the entire pressure range tested. The CO<sub>2</sub> uptake of MMC reached about 1.52 mmol g<sup>-1</sup> at 101 kPa and 0 °C (Table 7). In contrast, the CO<sub>2</sub> uptake under the same conditions on the purchased reference materials were at best 0.46 mmol g<sup>-1</sup> for MgO (Figure 11, right and Table 7). Note that N<sub>2</sub> adsorption and CO<sub>2</sub> desorption isotherms were too low to display in Figure 11 (right) and Figure 12 (right). The high CO<sub>2</sub> uptake on MMC is thought to be related to its high specific surface area (698 m<sup>2</sup> g<sup>-1</sup>, Table 2) and porosity (Figure 4, right), which allow CO<sub>2</sub> physisorption to take place extensively.

In Figure 11 to Figure 13 below, the N<sub>2</sub> adsorption isotherms are presented as red solid squares and the CO<sub>2</sub> adsorption isotherms as various solid black symbols for all materials. The CO<sub>2</sub> desorption isotherms are presented as hollow squares.

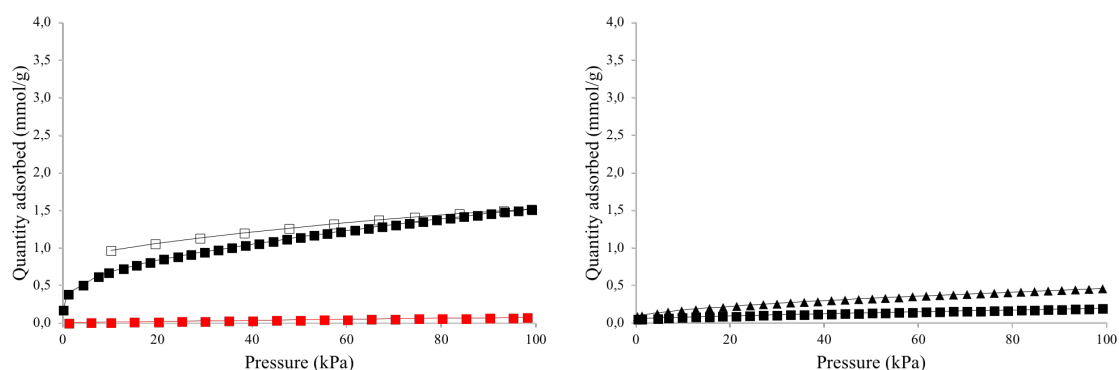


**Figure 11.** N<sub>2</sub> adsorption isotherms (red solid squares), CO<sub>2</sub> adsorption isotherms (solid black symbols) and CO<sub>2</sub> desorption isotherms (hollow symbols). MMC (Left), Sigma MgCO<sub>3</sub> (right; squares) and Sigma MgO (right; triangles).

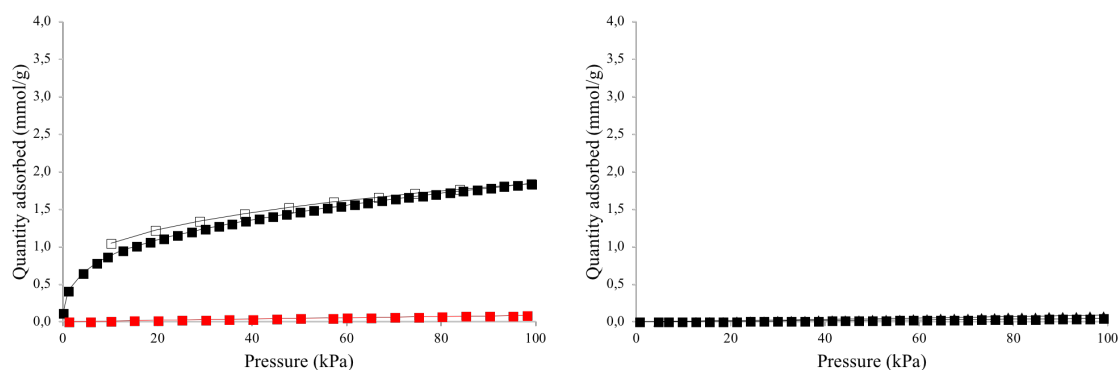


**Figure 12.** N<sub>2</sub> adsorption isotherms (red solid squares), CO<sub>2</sub> adsorption isotherms (solid black symbols) and CO<sub>2</sub> desorption isotherms (hollow symbols). MCC (Left), Sigma CaCO<sub>3</sub> (right; squares) and Alfa aesar CaO (right; triangles, covered).

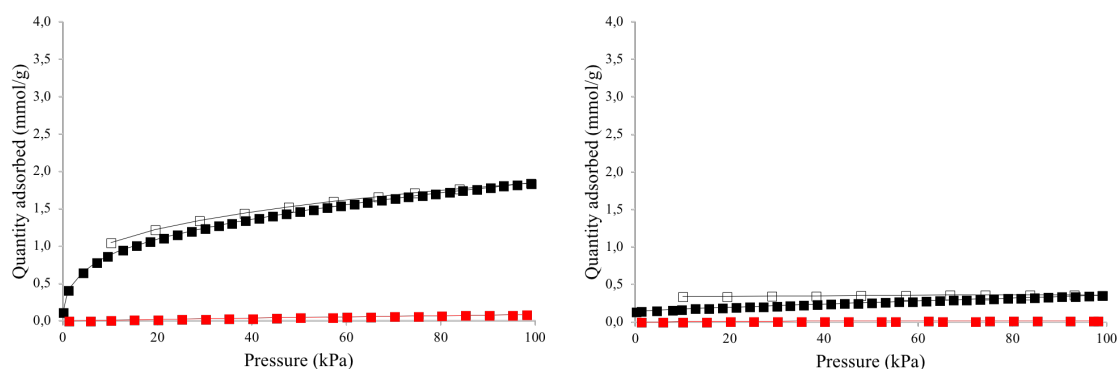


**Figure 13.** N<sub>2</sub> adsorption isotherms (red solid squares), CO<sub>2</sub> adsorption isotherms (solid black symbols) and CO<sub>2</sub> desorption isotherms (hollow symbols). MCC (Left) and Sigma synthetic hydrotalcite (Right).

### 3.3.2. CO<sub>2</sub> adsorption isotherms - Additives

The required energy for adsorption using solid adsorbents, would according to Songolzadeh et al. (2014), be less than 30-50 % of conventional chemical absorbents, such as an optimum aqueous monoethanolamine (MEA), if the CO<sub>2</sub> adsorption capacity reaches up to 3 mmol g<sup>-1</sup>. All of the tested additives on MMC appear to have positive effect on the CO<sub>2</sub> uptake with VSA (Table 7). However, the effects were the most profound when the additive 5 wt.% K<sub>2</sub>CO<sub>3</sub> was incorporated (for MMC-K<sub>2</sub>CO<sub>3</sub> 5 wt.%). The CO<sub>2</sub> uptake of this sample increased to 3.24 mmol g<sup>-1</sup> at 101 kPa (0 °C), as seen in Table 7 and Figure 16. This is over double that of as synthesized MMC (1.52 mmol g<sup>-1</sup>) under the same conditions (Table 7). Furthermore, this suggests that the required energy for adsorption using VSA on sample MMC-K<sub>2</sub>CO<sub>3</sub> 5 wt.%, due to the sorbents CO<sub>2</sub> capacity surpassing 3 mmol g<sup>-1</sup>, could be less than for conventional chemical absorbents (Songolzadeh et al., 2014).

The CO<sub>2</sub> uptake at 101 kPa (0 °C) for the various ratios of MCMC, seem to be higher with higher BET surface area, with MCMC 1:3 (2.76 mmol g<sup>-1</sup>) having the highest uptake of the ratios and the highest BET surface area (623 m<sup>2</sup> g<sup>-1</sup>, Table 7). The incorporation of aluminum to the MCMC structure indicates a decrease in BET surface area with increased weight percentages (Table 7). Furthermore, this reflects on the CO<sub>2</sub> uptake, which is also decreased (Figure 17 to Figure 19, right). All the base materials and additive materials had higher uptake than that of the purchased references using VSA (at 101 kPa, 0 °C). This is probably due to the additives inherent adsorption capabilities which could improve the base materials and allow physisorption to take place more extensively (2.1.3 Additives).

**Table 7.** CO<sub>2</sub> uptake using VSA (at 101 kPa, 0 °C) and the BET surface area of materials.

Sample name	BET surface area (m <sup>2</sup> g <sup>-1</sup> )	CO <sub>2</sub> uptake at 101 kPa, 0 °C
MMC	698	1.52
MMC-Al(NO <sub>3</sub> ) <sub>3</sub> 10 wt.%	518	1.90
MMC-Al <sub>2</sub> O <sub>3</sub> 10 wt.%	580	2.68
MMC-K <sub>2</sub> CO <sub>3</sub> 15 wt.%	490	2.20
MMC-K <sub>2</sub> CO <sub>3</sub> 10 wt.%	599	3.10
MMC-K <sub>2</sub> CO <sub>3</sub> 5 wt.%	637	3.24
MMC-KNO <sub>3</sub> 10 wt.%	499	2.15
MMC-KNO <sub>3</sub> 5 wt.%	563	2.49
MCC	394	1.84
MCMC 1:3	623	2.76
MCMC 1:2	539	2.12
MCMC 1:1	543	1.99
MCMC 2:1	572	2.68
MCMC 3:1	490	1.66
MCMC 3:1 Al 35 wt.%	306	0.76
MCMC 3:1 Al 25 wt.%	418	1.48
MCMC 3:1 Al 10 wt.%	501	1.69
Hydrotalcite	10	0.36
MgCO <sub>3</sub>	20	0.20
MgO	120	0.46
CaCO <sub>3</sub>	1	0.05
CaO	3	0.09

Additives on MMC appeared to have positive effect on the CO<sub>2</sub> uptake with VSA at all pressure ranges up to 101 kPa (0 °C) and the uptake of N<sub>2</sub> under the same conditions appeared to be unaffected by the additives (Figure 14 to Figure 16, red/purple solid squares). This is important when separating CO<sub>2</sub> from flue gas with a hypothetical gas mixture containing 15 vol.% CO<sub>2</sub> and 85 vol.% N<sub>2</sub>.

Presented in Figure 14 to Figure 16 are the CO<sub>2</sub> and N<sub>2</sub> adsorption isotherms (0 °C) of MMC with additives and MMC as reference. The highest CO<sub>2</sub> uptake was on the sample MMC-K<sub>2</sub>CO<sub>3</sub> 5 wt.%, already at relatively low pressures, reaching 1.5 mmol g<sup>-1</sup> at around 10 kPa and 3.24 mmol g<sup>-1</sup> at 101 kPa. That is more than double that of MMC at both pressures (0.7 and 1.52 mmol g<sup>-1</sup> respectively, Figure 16).

The CO<sub>2</sub> desorption isotherms presented as hollow squares, indicates that the samples are not completely regenerated by the vacuum, probably due to strongly physisorbed or chemisorbed CO<sub>2</sub> left on the surface. This will decrease the uptake of the samples for continuous cycles of VSA.

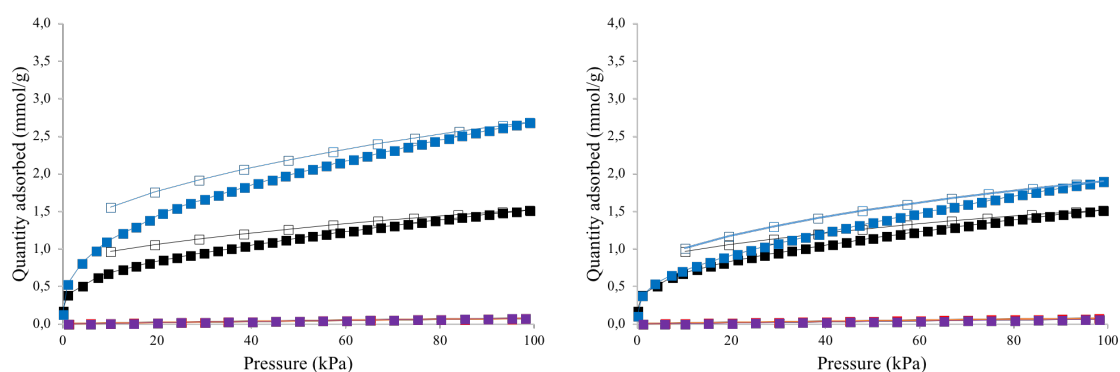


**Figure 14.** N<sub>2</sub> adsorption isotherms (red/purple solid squares), CO<sub>2</sub> adsorption isotherms (blue/black solid squares) and CO<sub>2</sub> desorption isotherms (hollow symbols) at 0 °C. MMC as reference (black/red squares). MMC-Al<sub>2</sub>O<sub>3</sub> 10 wt.% (Left; blue/purple squares) and MMC-Al(NO<sub>3</sub>)<sub>3</sub> 10 wt.% (right; blue/purple squares).

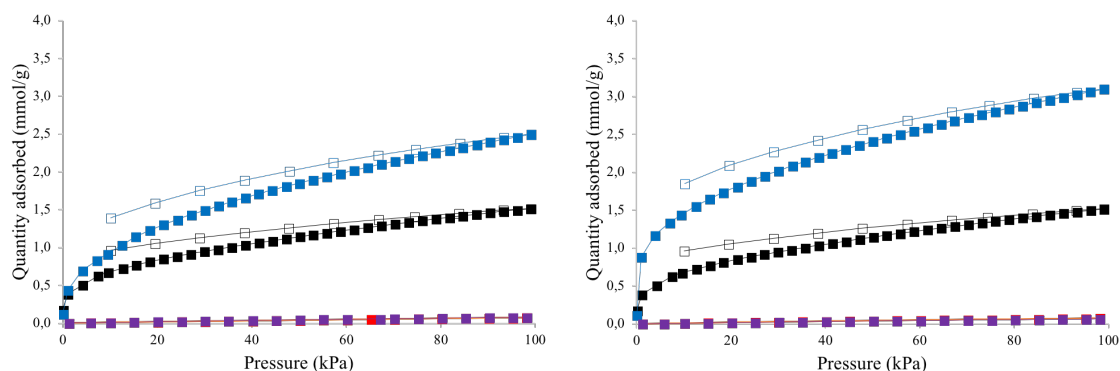


**Figure 15.** N<sub>2</sub> adsorption isotherms (red/purple solid squares), CO<sub>2</sub> adsorption isotherms (blue/black solid squares) and CO<sub>2</sub> desorption isotherms (hollow symbols) at 0 °C. MMC as reference (black/red squares). MMC-KNO<sub>3</sub> 5 wt.% (Left; blue/purple squares) and MMC-K<sub>2</sub>CO<sub>3</sub> 10 wt.% (right; blue/purple squares).

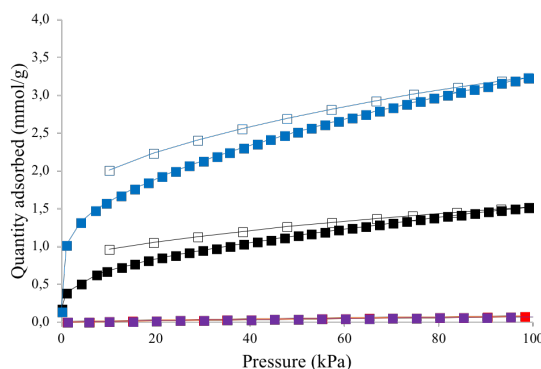


**Figure 16.** N<sub>2</sub> adsorption isotherms (red/purple solid squares), CO<sub>2</sub> adsorption isotherms (blue/black solid squares) and CO<sub>2</sub> desorption isotherms (hollow symbols) at 0 °C. MMC as reference (black/red squares) and MMC-K<sub>2</sub>CO<sub>3</sub> 5 wt.% (blue/purple squares).

With MCC as reference, below are the CO<sub>2</sub> and N<sub>2</sub> adsorption isotherms (0 °C) of the MCMC ratios (Figure 17 to Figure 19, left) and MCMC 3:1, with 10-35 wt.% of aluminum (Figure 17 to Figure 19, right), that have the highest uptake at 101 kPa.

As can be seen in Figure 18 and Figure 19 (left), MCMC 2:1 and 1:3 are the only materials of the MCMC ratios and aluminum additives that yield a higher CO<sub>2</sub> uptake at all pressure ranges compared to MCC. However, the N<sub>2</sub> uptake under the same conditions appear to be unaffected for all the ratios and additives.

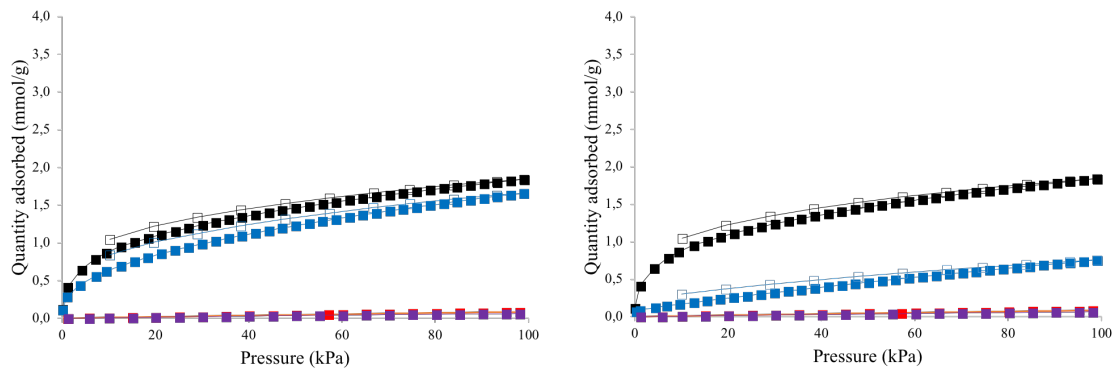


**Figure 17.** N<sub>2</sub> adsorption isotherms (red/purple solid squares), CO<sub>2</sub> adsorption isotherms (blue/black solid squares) and CO<sub>2</sub> desorption isotherms (hollow symbols) at 0 °C. MCC as reference (black/red squares). MCMC 3:1 (Left; blue/purple squares) and MCMC 3:1 Al 35 wt.% (right; blue/purple squares).

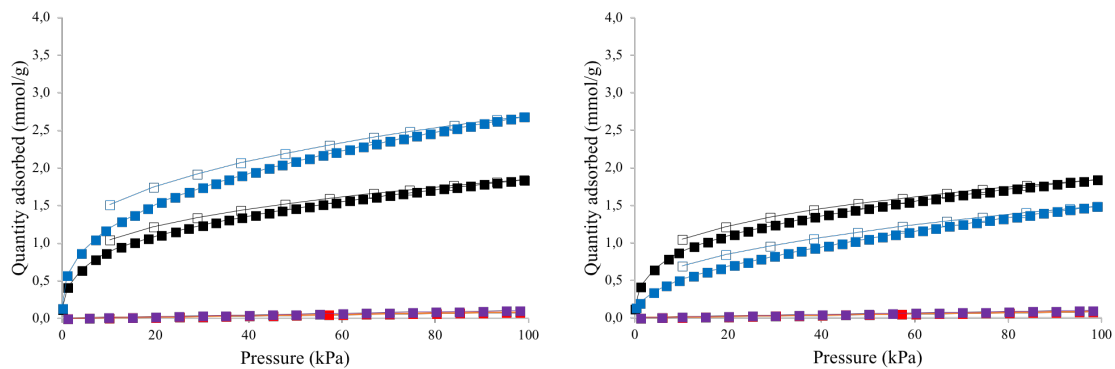


**Figure 18.** N<sub>2</sub> adsorption isotherms (red/purple solid squares), CO<sub>2</sub> adsorption isotherms (blue/black solid squares) and CO<sub>2</sub> desorption isotherms (hollow symbols) at 0 °C. MCC as reference (black/red squares). MCMC 2:1 (Left; blue/purple squares) and MCMC 3:1 Al 25 wt.% (right; blue/purple squares).

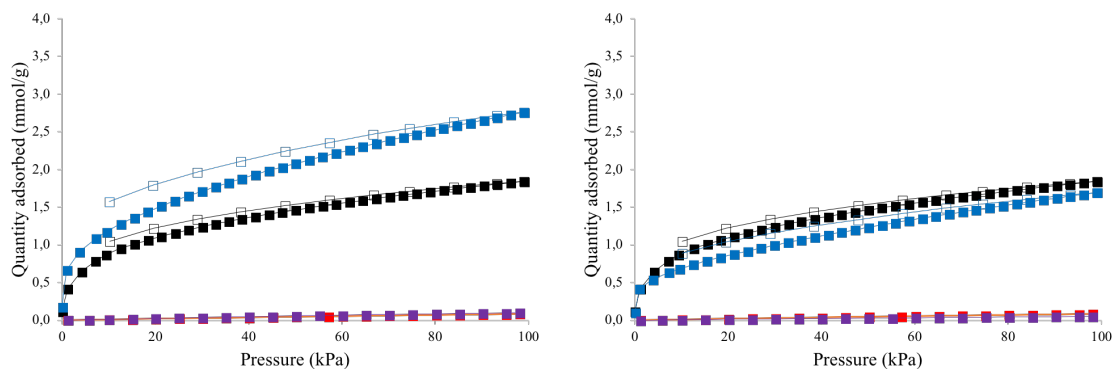


**Figure 19.** N<sub>2</sub> adsorption isotherms (red/purple solid squares), CO<sub>2</sub> adsorption isotherms (blue/black solid squares) and CO<sub>2</sub> desorption isotherms (hollow symbols) at 0 °C. MCC as reference (black/red squares). MCMC 1:3 (Left; blue/purple squares) and MCMC 3:1 Al 10 wt.% (right; blue/purple squares).

### 3.3.3. CO<sub>2</sub> vacuum swing cycling

Three of the samples with the highest CO<sub>2</sub> uptake at 101 kPa (0°C) using VSA were tested for cyclic stability and capacity (MMC-K<sub>2</sub>CO<sub>3</sub> 5 wt.%, MMC-Al<sub>2</sub>O<sub>3</sub> 10 wt.% and MCMC 1:3, Table 7). Figure 20 presents the samples CO<sub>2</sub> uptake over four cycles with vacuum regeneration.

As seen in Figure 14 to Figure 19, the CO<sub>2</sub> desorption isotherms show an uncompleted regeneration by vacuum, probably leaving strongly physisorbed or chemisorbed CO<sub>2</sub> on the surface. This is probably why the samples in Figure 20 have a decrease in CO<sub>2</sub> adsorption each cycle.

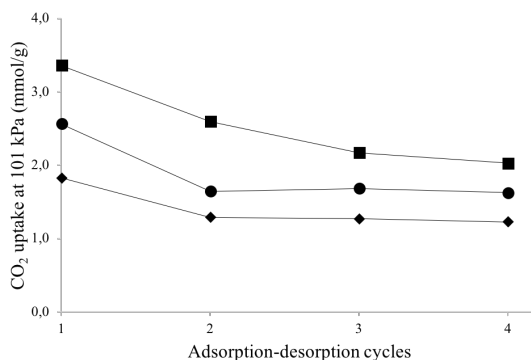


**Figure 20.** Cyclic CO<sub>2</sub> uptake at 101 kPa and 0 °C of MMC-K<sub>2</sub>CO<sub>3</sub> 5 wt.% (squares), MMC-Al<sub>2</sub>O<sub>3</sub> 10 wt.% (circles) and MCMC 1:3 (diamonds) with vacuum regeneration.

### 3.4. CO<sub>2</sub> CYCLING AT ROOM TEMPERATURE

Vacuum swing cyclic CO<sub>2</sub> adsorption/desorption showed that the CO<sub>2</sub> uptake on MMC with 5 wt.% K<sub>2</sub>CO<sub>3</sub> decreased after each cycle (Figure 20). This was thought to be due to the vacuum not being able to completely regenerate the sample. This probably leaves strongly physisorbed or chemisorbed CO<sub>2</sub> on the surface of the material that could be heat regenerated. Using TSA, cyclic CO<sub>2</sub> adsorption at room temperature and a regeneration temperature of 150 °C (30 min) was applied to the sample MMC-K<sub>2</sub>CO<sub>3</sub> 5 wt.%, to see if it was possible to recover most of the lost CO<sub>2</sub> capacity after each cycle (Figure 21). The initial CO<sub>2</sub> uptake (1<sup>st</sup> cycle) was decreased to 2.43 mmol g<sup>-1</sup> compared to VSA experiments (3.24 mmol g<sup>-1</sup>). This is probably due to the adsorption temperature being at RT (25 °C), which is the minimum temperature for TSA experiments. It could also be due to the sample being heated to 150 °C for 2 hours prior to the first cycle, perhaps changing the material structure. However, SEM micrographs show no visual changes to the nanostructure (3.1 Characterization, Figure 24). With the low decrease in the CO<sub>2</sub> uptake each cycle, seen in Figure 21, heat regeneration indicatively improved the cyclic performance of MMC-K<sub>2</sub>CO<sub>3</sub> 5 wt.% compared to vacuum regeneration of the same adsorbent (Figure 20). This suggests a good thermal and cyclic stability for this temperature range and material composition.

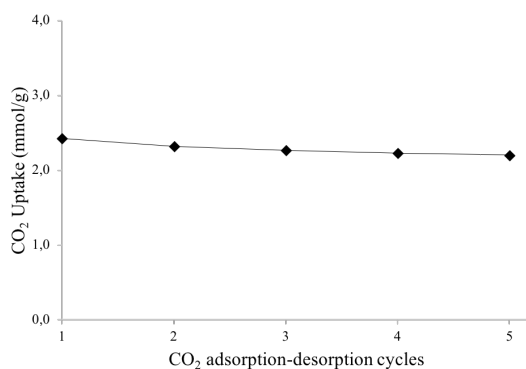


**Figure 21.** Cyclic CO<sub>2</sub> uptake at room temperature of MMC-K<sub>2</sub>CO<sub>3</sub> 5 wt.% with heat regeneration (150 °C).

### 3.5. THERMAL STABILITY AND SINTERING

The incorporation of 5 wt.% of K<sub>2</sub>CO<sub>3</sub> on MMC (for MMC-K<sub>2</sub>CO<sub>3</sub> 5 wt.%) was shown to have a profound effect on the CO<sub>2</sub> uptake using vacuum swing adsorption. The CO<sub>2</sub> uptake increased to 3.24 mmol g<sup>-1</sup> at 101 kPa (0 °C), over double that of MMC (1.52 mmol g<sup>-1</sup>) without additives, under the same conditions (Table 7). Adding K<sub>2</sub>CO<sub>3</sub> to MMC did not change the structure of the material as seen from the SEM micrograph of MMC-K<sub>2</sub>CO<sub>3</sub> 5 wt.% in Figure 22 (right). Additive compositions for all additive materials and their BET specific surface area listed in Table 3. Powder XRD pattern of MMC-K<sub>2</sub>CO<sub>3</sub> 5 wt.% (Figure 22, left) showed that MMC remained amorphous, with minor diffraction peaks related to the additive itself.

SEM micrographs of MMC-K<sub>2</sub>CO<sub>3</sub> 5 wt.% (Figure 23) after CO<sub>2</sub> vacuum swing adsorption, show that the physisorption of CO<sub>2</sub> molecules on the material surface did not change the nanostructure of the sample.

The high uptake of MMC-K<sub>2</sub>CO<sub>3</sub> 5 wt.% (VSA, at 101 kPa, 0°C) was shown to decrease for every vacuum swing cycle (Figure 20), probably due to strongly physisorbed or chemisorbed CO<sub>2</sub> left on the surface. Heat regeneration (150 °C) under N<sub>2</sub> flow for 30 minutes could be used to improve the cyclic performance (Figure 21) and the SEM micrographs (Figure 24) show no structural change of the material after 5 cycles.

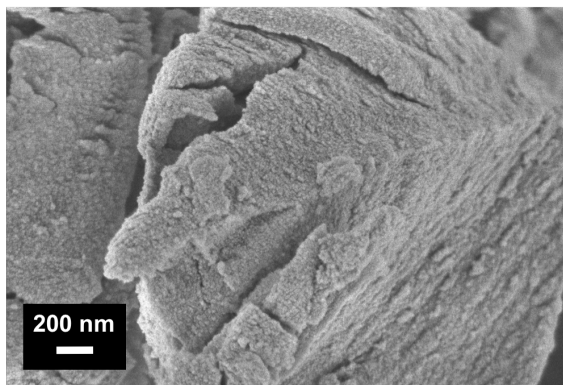
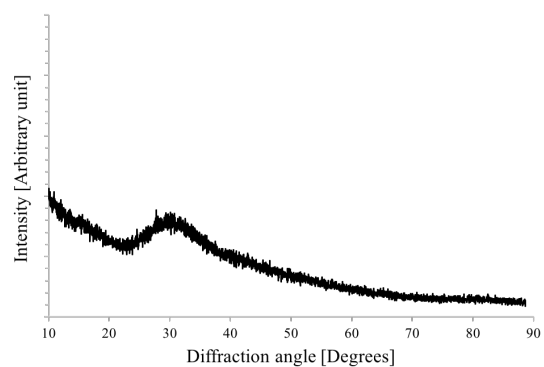


**Figure 22.** Powder X-ray diffraction (left) and SEM micrograph (right) of as synthesized MMC-K<sub>2</sub>CO<sub>3</sub> 5 wt.%.

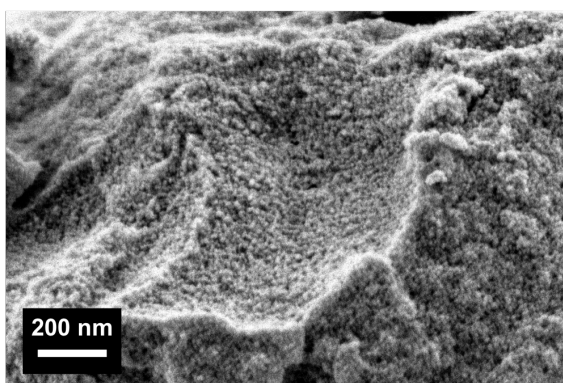
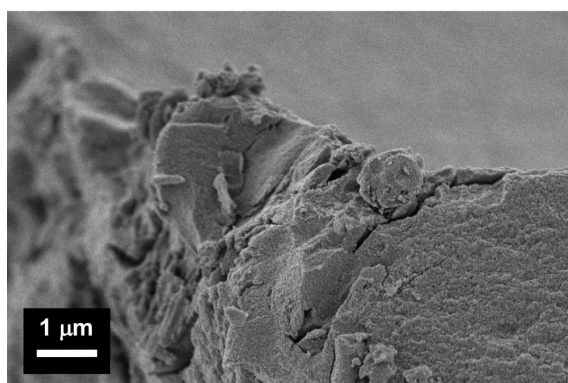


**Figure 23.** SEM micrographs of MMC-K<sub>2</sub>CO<sub>3</sub> 5 wt.% after CO<sub>2</sub> vacuum swing adsorption.

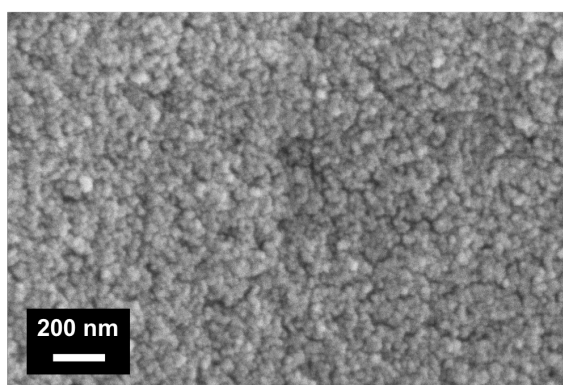
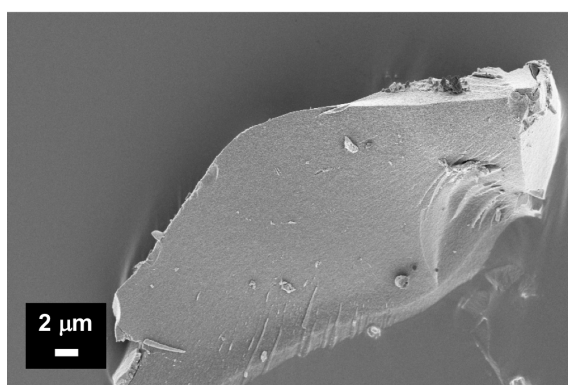


**Figure 24.** SEM micrographs of MMC-K<sub>2</sub>CO<sub>3</sub> 5 wt.% after 5 cycles of CO<sub>2</sub> temperature swing adsorption at room temperature (25 °C) and heat regeneration (150 °C).

As seen in the XRD pattern in Figure 25 (left), adding 35 wt.%  $\text{Al}(\text{NO}_3)_3$  to MCMC 3:1, the material remained amorphous, with minor diffraction peaks related to aluminum. The SEM micrograph (Figure 25, right) show a remaining nanoporous structure after the addition of aluminum.

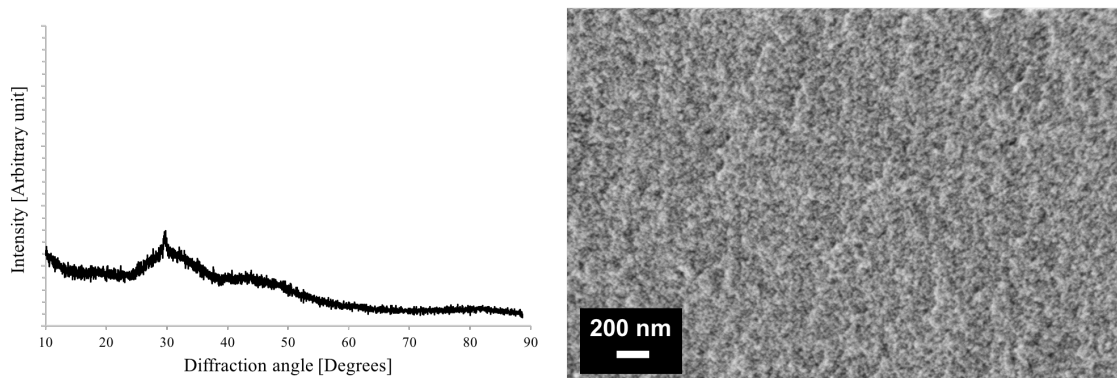


**Figure 25.** Powder X-ray diffraction (left) and SEM micrograph (right) of as synthesized MCMC 3:1 Al 35 wt.%.

Through measurements with ASAP, it was found that the porosity of the regenerated MCMC was changing with cyclic numbers and is thought to be attributed to the formation of large single CaO crystals. Previous studies has shown that the change in porosity is a conversion from a loss of small pores to an increase of large pores (Li et al., 2006).

SEM micrographs of MCC after 23 TSA cycles (850-650 °C) show sintering to a great extent (Figure 26), with the formation of large pores and the destruction of its nanoporous structure (original nanoporous structure, Figure 5, right). Furthermore, SEM micrographs of MCMC 3:1 after 23 cycles of TSA (850-650 °C) clearly show the sintering of MCMC into dough-like formations distinctly shown in Figure 27 (bottom right), similar to that of MCC but limited to small regions. This sintering was seen to an even lesser extent with the addition of 35 wt.%  $\text{Al}(\text{NO}_3)_3$  on MCMC (for MCMC 3:1 Al 35 wt.%) depicted in Figure 28. This is further reinforced by the uptake of MCMC 3:1 Al 35 wt.% after 23 cycles (10.96 mmol  $\text{g}^{-1}$ ) compared to MCMC 3:1 (8.56 mmol  $\text{g}^{-1}$ ) and MCC (7.29 mmol  $\text{g}^{-1}$ ) with the same cyclic TSA in the 650-850 °C temperature range (Figure 7).

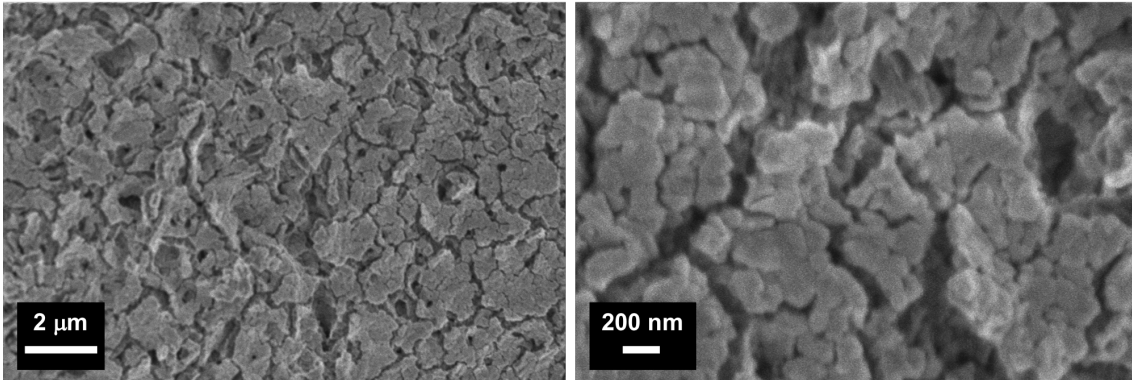


**Figure 26.** SEM micrographs of MCC after 23 cycles of CO<sub>2</sub> temperature swing adsorption (850-650 °C).

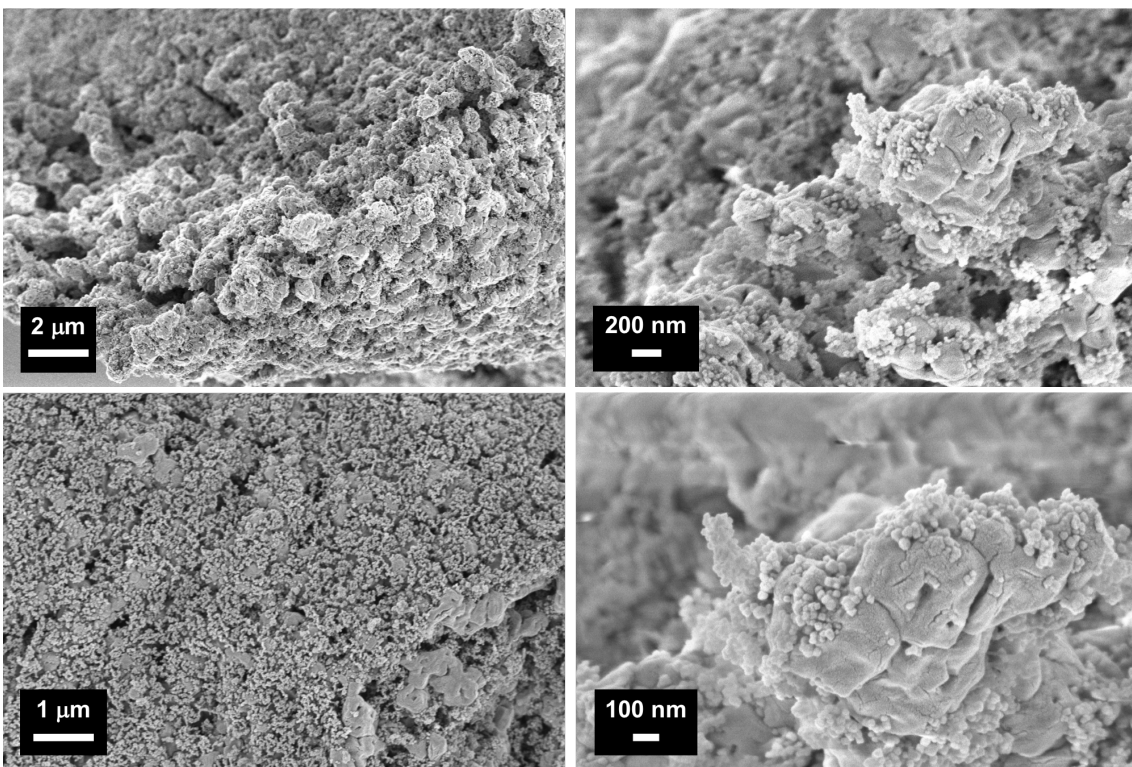


**Figure 27.** SEM micrographs of MCMC 3:1 after 23 cycles of CO<sub>2</sub> temperature swing adsorption (850-650 °C).

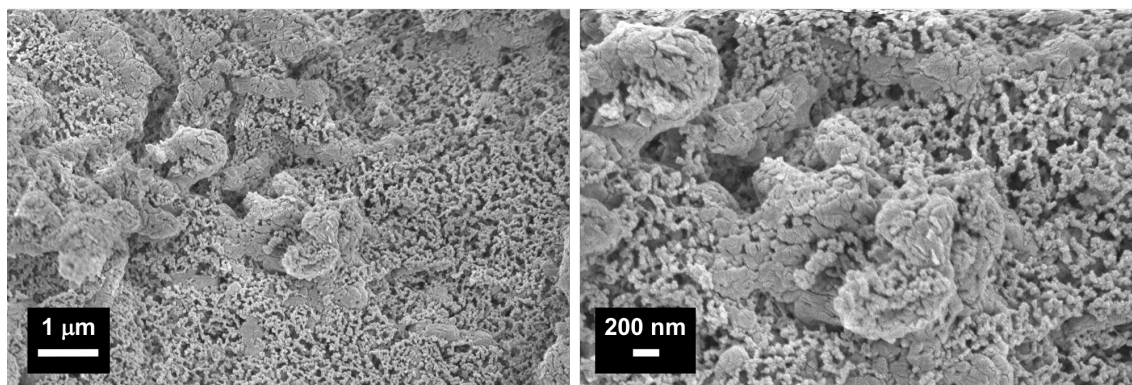


**Figure 28.** SEM micrographs of MCMC 3:1 Al 35 wt.% after 23 cycles of CO<sub>2</sub> temperature swing adsorption (850-650 °C).

## 4. CONCLUSIONS

### 4.1. Characterization

MIC with high porosity and surface area (up to 700 m<sup>2</sup> g<sup>-1</sup>) was successfully synthesized with additives and characterized by BET, XRD and SEM analysis. MIC was optimized and tested as potential CO<sub>2</sub> adsorbents in CO<sub>2</sub> separation. MIC with additives remained X-ray amorphous as well as nanoporous, with a small decrease in BET surface area with higher weight percentages of additives.

### 4.2. Temperature swing adsorption

CO<sub>2</sub> adsorption capacity was measured using temperature swing adsorption at the temperature ranges 200-450 °C and 650-850 °C. Higher amounts of additives decreased the CO<sub>2</sub> adsorption capacity and adsorption kinetics of the samples tested, but with an overall increase of thermal and cyclic stability. MCC had a relatively high CO<sub>2</sub> uptake, which was drastically lowered by severe sintering after continuous TSA cycles, when heat was used as the method of adsorbent regeneration. The combined structure of MCMC improved the thermal and cyclic stability, mitigating the sintering. The addition of Al(NO<sub>3</sub>)<sub>3</sub> improved the thermal and cyclic stability further, with an optimum additive amount of 35 wt.% aluminum.

MCMC 3:1 Al 35 wt.% was the best performing sample using TSA, in regard to CO<sub>2</sub> uptake, thermal and cyclic stability, with an initial CO<sub>2</sub> uptake of 12.23 mmol g<sup>-1</sup> and 10.96 mmol g<sup>-1</sup> at the 23<sup>rd</sup> cycle.

### 4.3. Vacuum swing adsorption

CO<sub>2</sub> adsorption capacity was measured at 0 °C from 0 to 101 kPa using vacuum swing adsorption. Additives on MIC had positive effect on the CO<sub>2</sub> uptake at all pressure ranges and the uptake of N<sub>2</sub> under the same conditions appeared to be unaffected by the additives. CO<sub>2</sub> adsorption capacity for MIC with additives, seemed to be higher with higher BET surface area and porosity, probably allowing CO<sub>2</sub> physisorption to take place more extensively. MMC had a good level of CO<sub>2</sub> uptake (1.52 mmol g<sup>-1</sup>) and a low N<sub>2</sub> uptake under the same conditions. MMC containing 5 wt. % of K<sub>2</sub>CO<sub>3</sub> as an additive, adsorbed

more than twice as much CO<sub>2</sub> (3.24 mmol g<sup>-1</sup>) under the same conditions when compared with as synthesized MMC.

MMC-K<sub>2</sub>CO<sub>3</sub> 5 wt.% was the best performing adsorbent in this work using VSA. Furthermore, this derives that the required energy for adsorption using VSA on sample MMC-K<sub>2</sub>CO<sub>3</sub> 5 wt.%, due to the sorbents CO<sub>2</sub> capacity surpassing 3 mmol g<sup>-1</sup>, could be less than for conventional chemical absorbents.

Cyclic CO<sub>2</sub> adsorption experiments showed that the CO<sub>2</sub> uptake capacity decreased with each cycle when vacuum was used as the adsorbent regeneration method. Probably leaving strongly physisorbed or chemisorbed CO<sub>2</sub> on the surface. Heat regeneration of 150 °C under N<sub>2</sub> flow for 30 minutes improved the cyclic performance of MMC with 5 wt.% K<sub>2</sub>CO<sub>3</sub>. This suggests a good thermal and cyclic stability for the sample in the temperature range 25-150 °C. MMC-K<sub>2</sub>CO<sub>3</sub> could be further developed as an adsorbent for CO<sub>2</sub> separation using temperature swing adsorption techniques.

## 5. FUTURE OUTLOOK

The results in this work could be used to further optimize adsorption techniques for CO<sub>2</sub> separation in exhaust gas in various industries. Effective adsorbents could be utilized to reduce the required energy in carbon capture processes and to mitigate the increasing carbon dioxide in the atmosphere, thereby reducing the weather extremes of climate change. The results in this work are a small part of a large effort in the scientific and engineering community to mitigate global CO<sub>2</sub> emissions. Hopefully adsorption technologies can be developed further to produce an effective alternative to existing absorption processes.

Experiments performed in this work was conducted in a lab environment, made to enact point sources. In practice, point sources are much larger, emitting extensive amounts of CO<sub>2</sub>. As a first step in optimizing MIC as adsorbents, some progress has been made, but much work remains to be done in this field.

MMC with the addition of K<sub>2</sub>CO<sub>3</sub> could be further developed as an adsorbent for CO<sub>2</sub> separation using temperature swing adsorption methods. MCMC could be further optimized with lower ratios of calcium and the addition of potassium or aluminum for CO<sub>2</sub> adsorption in the low and intermediate temperature ranges.

## 6. REFERENCES

- Bacsik, Z., Cheung, O., Vasiliev, P., Hedin, N., 2016. Selective separation of CO<sub>2</sub> and CH<sub>4</sub> for biogas upgrading on zeolite NaKA and SAPO-56. *Appl. Energy* 162, 613–621. <https://doi.org/10.1016/j.apenergy.2015.10.109>
- Bhatta, L.K.G., Subramanyam, S., Chengala, M.D., Olivera, S., Venkatesh, K., 2015. Progress in hydrotalcite like compounds and metal-based oxides for CO<sub>2</sub> capture: a review. *J. Clean. Prod., Carbon Emissions Reduction: Policies, Technologies, Monitoring, Assessment and Modeling* 103, 171–196. <https://doi.org/10.1016/j.jclepro.2014.12.059>
- Brunauer, S., Emmett, P.H., Teller, E., 1938. Adsorption of Gases in Multimolecular Layers. *J. Am. Chem. Soc.* 60, 309–319. <https://doi.org/10.1021/ja01269a023>
- Buhre, B.J.P., Elliott, L.K., Sheng, C.D., Gupta, R.P., Wall, T.F., 2005. Oxy-fuel combustion technology for coal-fired power generation. *Prog. Energy Combust. Sci.* 31, 283–307. <https://doi.org/10.1016/j.pecs.2005.07.001>
- Chen, C., Ahn, W.-S., 2011. CO<sub>2</sub> capture using mesoporous alumina prepared by a sol-gel process. *Chem. Eng. J.* 166, 646–651. <https://doi.org/10.1016/j.cej.2010.11.038>
- Cheung, O., Zhang, P., Frykstrand, S., Zheng, H., Yang, T., Sommariva, M., Zou, X., Strømme, M., 2016. Nanostructure and pore size control of template-free synthesised mesoporous magnesium carbonate. *RSC Adv.* 6, 74241–74249. <https://doi.org/10.1039/C6RA14171D>
- Field, C.B., Barros, V.R., Intergovernmental Panel on Climate Change (Eds.), 2014. *Climate change 2014: impacts, adaptation, and vulnerability: Working Group II contribution to the fifth assessment report of the Intergovernmental Panel on Climate Change.* Cambridge University Press, New York, NY.
- Fogarty, J., McCally, M., 2010. Health and Safety Risks of Carbon Capture and Storage. *JAMA* 303, 67–68. <https://doi.org/10.1001/jama.2009.1951>
- Forsgren, J., Frykstrand, S., Grandfield, K., Mihranyan, A., Strømme, M., 2013. A Template-Free, Ultra-Adsorbing, High Surface Area Carbonate Nanostructure. *PLOS ONE* 8, e68486. <https://doi.org/10.1371/journal.pone.0068486>
- Haaf, M., Stroh, A., Hilz, J., Helbig, M., Ströhle, J., Epple, B., 2017. Process Modelling of the Calcium Looping Process and Validation Against 1 MWth Pilot Testing. *Energy Procedia, 13th International Conference on Greenhouse Gas Control Technologies, GHGT-13, 14-18 November 2016, Lausanne, Switzerland* 114, 167–178. <https://doi.org/10.1016/j.egypro.2017.03.1159>
- Hilz, J., Helbig, M., Haaf, M., Daikeler, A., Ströhle, J., Epple, B., 2018. Investigation of the fuel influence on the carbonate looping process in 1 MWth scale. *Fuel Process. Technol.* 169, 170–177. <https://doi.org/10.1016/j.fuproc.2017.09.016>
- Juho, L., 2015. Storing CO<sub>2</sub> through Enhanced Oil Recovery 48.
- Karplus, M., Kolker, H.J., 1964. Van der Waals Forces in Atoms and Molecules. *J. Chem. Phys.* 41, 3955–3961. <https://doi.org/10.1063/1.1725842>
- Li, Z.-S., Cai, N.-S., Huang, Y.-Y., 2006. Effect of preparation temperature on cyclic CO<sub>2</sub> capture and multiple carbonation-calcination cycles for a new Ca-based CO<sub>2</sub> sorbent. *Ind. Eng. Chem. Res.* 45, 1911–1917. <https://doi.org/10.1021/ie0512111>
- Songolzadeh, M., Soleimani, M., Takht Ravanchi, M., Songolzadeh, R., 2014. Carbon Dioxide Separation from Flue Gases: A Technological Review Emphasizing Reduction in Greenhouse Gas Emissions [WWW Document]. *Sci. World J.* <https://doi.org/10.1155/2014/828131>

- Wagner, L., Ross, I., Foster, J., Hankamer, B., 2016. Trading Off Global Fuel Supply, CO<sub>2</sub> Emissions and Sustainable Development. PLOS ONE 11, e0149406. <https://doi.org/10.1371/journal.pone.0149406>
- Wall, T.F., 2007. Combustion processes for carbon capture. Proc. Combust. Inst. 31, 31–47. <https://doi.org/10.1016/j.proci.2006.08.123>
- Walspurger, S., Boels, L., Cobden, P.D., Elzinga, G.D., Haije, W.G., van den Brink, R.W., 2008. The crucial role of the K<sup>+</sup>-aluminium oxide interaction in K<sup>+</sup>-promoted alumina- and hydrotalcite-based materials for CO<sub>2</sub> sorption at high temperatures. ChemSusChem 1, 643–650. <https://doi.org/10.1002/cssc.200800085>
- Wang, M., Lawal, A., Stephenson, P., Sidders, J., Ramshaw, C., 2011. Post-combustion CO<sub>2</sub> capture with chemical absorption: A state-of-the-art review. Chem. Eng. Res. Des., Special Issue on Carbon Capture & Storage 89, 1609–1624. <https://doi.org/10.1016/j.cherd.2010.11.005>
- Wang, S., Yan, S., Ma, X., Gong, J., 2011. Recent advances in capture of carbon dioxide using alkali-metal-based oxides. Energy Environ. Sci. 4, 3805–3819. <https://doi.org/10.1039/c1ee01116b>
- Webley, P.A., Qader, A., Ntiamoah, A., Ling, J., Xiao, P., Zhai, Y., 2017. A New Multi-bed Vacuum Swing Adsorption Cycle for CO<sub>2</sub> Capture from Flue Gas Streams. Energy Procedia, 13th International Conference on Greenhouse Gas Control Technologies, GHGT-13, 14-18 November 2016, Lausanne, Switzerland 114, 2467–2480. <https://doi.org/10.1016/j.egypro.2017.03.1398>
- Xiao, G., Singh, R., Chaffee, A., Webley, P., 2011. Advanced adsorbents based on MgO and K<sub>2</sub>CO<sub>3</sub> for capture of CO<sub>2</sub> at elevated temperatures. Int. J. Greenh. Gas Control 5, 634–639. <https://doi.org/10.1016/j.ijggc.2011.04.002>